Curr Genet (2018) 64:599–617
DOI 10.1007/s00294-017-0776-6

ORIGINAL ARTICLE

Interaction of the *Saccharomyces cerevisiae* RING-domain protein Nse1 with Nse3 and the Smc5/6 complex is required for chromosome replication and stability

Saima Wani[1] · Neelam Maharshi[1] · Deepash Kothiwal[1] · Lakshmi Mahendrawada[1] · Raju Kalaivani[2] · Shikha Laloraya[1]

Received: 25 October 2017 / Revised: 27 October 2017 / Accepted: 31 October 2017 / Published online: 8 November 2017

Abstract Genomic stability is maintained by the concerted actions of numerous protein complexes that participate in chromosomal duplication, repair, and segregation. The Smc5/6 complex is an essential multi-subunit complex crucial for repair of DNA double-strand breaks. Two of its subunits, Nse1 and Nse3, are homologous to the RING-MAGE complexes recently described in human cells. We investigated the contribution of the budding yeast Nse1 RING-domain by isolating a mutant *nse1-103* bearing substitutions in conserved Zinc-coordinating residues of the RING-domain that is hypersensitive to genotoxic stress and temperature. The nse1-103 mutant protein was defective in interaction with Nse3 and other Smc5/6 complex subunits, Nse4 and Smc5. Chromosome loss was enhanced, accompanied by a delay in the completion of replication and a modest defect in sister chromatid cohesion, in *nse1-103*. The *nse1-103* mutant was synthetic sick with *rrm3*Δ (defective in fork passage through pause sites), this defect was rescued by inactivation of Tof1, a subunit of the fork protection complex that enforces pausing. The temperature sensitivity of *nse1-103* was partially suppressed by deletion of *MPH1*, encoding a DNA-helicase. Homology modeling of the structure of the budding yeast Nse1–Nse3 heterodimer based on the human Nse1–MAGEG1 structure suggests a similar organization and indicates that perturbation of the Zn-coordinating cluster has the potential to allosterically alter structural elements at the Nse1/Nse3 interaction interface that may abrogate their association. Our findings demonstrate that the budding yeast Nse1 RING-domain organization is important for interaction with Nse3, which is crucial for completion of chromosomal replication, cohesion, and maintenance of chromosome stability.

Keywords Chromosome stability · DNA replication · Mitosis · Molecular genetics · Protein–protein interaction · Yeast two-hybrid

Abbreviations

Smc	Structural maintenance of chromosomes
MMS	Methyl methane sulfonate
HU	Hydroxyurea
Mms21	MMS-sensitive 21
SUMO	Small ubiquitin-related modifier
Nse	Non-smc element
DSB	Double-strand break
GCR	Gross chromosomal rearrangements
GST	Glutathione S-transferase
MAGEG1	Melanoma antigen G1
MPH1	Mutator Phenotype
PFGE	Pulsed-field gel electrophoresis
Rad	Radiation-sensitive
rDNA	Ribosomal DNA
RING	Really interesting new gene
Rrm3	rDNA recombination mutation 3
Tof1	Topoisomerase I-interacting Factor 1
YPD	Yeast extract–peptone–dextrose

Communicated by M. Kupiec.

Electronic supplementary material The online version of this article (https://doi.org/10.1007/s00294-017-0776-6) contains supplementary material, which is available to authorized users.

✉ Shikha Laloraya
slaloraya@iisc.ac.in

[1] FE13, New Biological Sciences Building, Department of Biochemistry, Indian Institute of Science, C. V. Raman Avenue, Bangalore, Karnataka 560012, India

[2] Molecular Biophysics Unit, Indian Institute of Science, C. V. Raman Avenue, Bangalore, Karnataka 560012, India

SC	Synthetic complete medium
YAC	Yeast artificial chromosome
5-FOA	5-fluoroorotic acid

Introduction

Maintenance of chromosome stability during cell division is crucial for the transmission of genetic information to daughter cells. During mitotic divisions, DNA is duplicated completely in S-phase of the cell cycle and segregated equally in M-phase to ensure the inheritance of a complete and unaltered copy of the genome. Several complex mechanisms operate to ensure that these processes are error-free such that daughter cells can inherit the full chromosome complement. A defect in any step of genome duplication and partitioning can result in chromosomal aberrations, such as aneuploidy or gross chromosomal rearrangements (GCRs), often observed in some human development disorders associated with chromosome abnormalities and in cancer cells (Hartwell and Kastan 1994; Putnam et al. 2016).

The fidelity of inheritance of genetic information is maintained by mechanisms ensuring that DNA replication does not produce heritable changes for which the DNA replication machinery has to be accurate and surveillance mechanisms detect and correct errors. The surveillance mechanisms include repair systems that can remove mismatched bases replacing them with correct ones, detect the presence of DNA ss (single-strand) or ds (double-strand) breaks or other lesions and repair them, or rescue stalled or collapsed replication forks such that replication can resume (Branzei and Foiani 2009, 2010). After completion of DNA replication, the two resultant DNA molecules, also termed sister-chromatids have to be partitioned accurately between the two daughter cells formed by mitotic division.

SMC (Structural maintenance of chromosomes) proteins are important for chromosome structural alterations that facilitate equal segregation during mitosis (Jeppsson et al. 2014). SMC protein complexes are conserved essential protein complexes that bind chromosomes and are involved in various chromosomal processes (Jeppsson et al. 2014; Koshland and Strunnikov 1996; Losada and Hirano 2005; Matityahu and Onn 2017; Uhlmann 2016). Cohesin (Ding et al. 2016; Rankin and Dawson 2016; Skibbens 2016) and Condensin (Hirano 2016; Iwasaki and Noma 2016; Robellet et al. 2016) are two conserved Smc protein complexes required for sister-chromatid cohesion and mitotic chromosome condensation that are important for chromosome stability. A third SMC-complex, the Smc5/6 complex, is conserved from bacteria to humans and all its subunits are essential for viability (De Piccoli et al. 2009). Cells having mutations in Smc5/6 complex subunits are sensitive to genotoxic stressors [e.g. methyl methane sulfonate (MMS), hydroxyurea (HU) etc.] that cause DNA damage, such as DNA double-strand breaks (DSBs) and stalled or collapsed replication forks. The Smc5/6 complex is recruited to sites of DNA damage and is required for DSB repair by Sister Chromatid Recombination (SCR) (De Piccoli et al. 2006). There is also mounting evidence for a role of the Smc5/6 complex in the recovery of collapsed replication forks. In both fission and budding yeasts, Smc5/6 complex is recruited to collapsed replication forks where it may promote their recovery and hence maintenance of genomic stability (Ampatzidou et al. 2006; Lindroos et al. 2006).

In eukaryotes, the Smc5/6 complex has eight subunits; Smc5 and Smc6 form a heterodimer and associate with six Nse (Non smc element) subunits, Nse1-6. The Smc5 and Smc6 proteins have a structure that is typical of Smc proteins including an ATP-binding head domain, two coiled coil regions and a hinge region, and they associate with each other by the hinge region. In budding yeast, Nse5 and Nse6 associate with the hinge region of the Smc5/6 heterodimer (Duan et al. 2009b). Nse1, 3 and 4 form a trimeric complex that binds the head domain of Smc5. Nse2, also known as Mms21, binds to the coiled coil region of Smc5 (Duan et al. 2009a).

The functions of these Nse subunits are being investigated—some of them modulate the function of the Smc5/6 complex in DNA damage repair by affecting its recruitment to DNA lesions or by participating in its function. For example, the Nse5/6 sub-complex is important for resolution of Holliday junction intermediates during meiotic recombination (Wehrkamp-Richter et al. 2012). Furthermore, Nse6 binds RTT107/Esc4, a BRCT domain-containing protein that is required for the recruitment of Smc5/6 to DNA DSBs (Leung et al. 2011). Recruitment of Smc6 to stalled forks is also reduced in *nse5* mutants, which also show replisome instability and accumulation of X-shaped DNA structures in the presence of HU-induced replication stress (Bustard et al. 2012). An intriguing and well-characterized subunit is Nse2/Mms21, a SUMO E3 ligase (Zhao and Blobel 2005) that sumoylates a number of chromosomal and DNA repair proteins. SUMO ligase domain-defective *mms21* mutants are hypersensitive to DNA damaging agents indicating a role for Mms21-mediated sumoylation in recovery from extrinsically induced DNA damage (Prakash and Prakash 1977; Rai et al. 2011). These mutants are also slow growing and display mitotic progression defects and chromosome instability (Mahendrawada et al. 2017; Rai and Laloraya 2017; Rai et al. 2011). Inactivation of the SUMO ligase activity of Mms21 also results in the accumulation of X-molecules at damaged replication forks in MMS-treated cells in a Rad51-dependent manner (Branzei et al. 2006); formation of such intermediates is also observed in *sgs1Δ* cells deficient in Sgs1/BLM, a sumoylation target of Mms21 (Bermudez-Lopez and Aragon 2017).

Relatively little is known yet about the Nse1, 3 and 4 trimeric complex, although based on structural predictions, Nse4 is a member of the kleisin family of Smc-associated proteins (e.g. Mcd1/Scc1 in the cohesin complex) that bridge the head domains of Smc subunits (Palecek et al. 2006). Nse3 and Nse1 are related to the MAGE–RING complexes recently described in human cells and share significant similarity to the MAGEG1–NSE1 complex that was demonstrated to have ubiquitin ligase activity *in vitro* (Doyle et al. 2010). Nse1 has been well studied in fission yeast and to a lesser extent in budding yeast. Fission yeast Nse1 (SpNse1) was found associated with Smc5 and Smc6, and is essential and epistatic to rhp51 in its requirement for resistance to damage induced by UV and gamma rays (McDonald et al. 2003). SpNse1 RING mutants are sensitive to genotoxic stress and are defective in interaction with Nse4 and recruitment of Smc5 and Nse4 to damage-induced sub-nuclear foci (Pebernard et al. 2008). In another study (Tapia-Alveal and O'Connell 2011), mutation in conserved cysteines in the RING domain resulted in reduction of binding of Nse4 to various loci potentially containing lesions induced by MMS and HU. Interestingly, a RING-mutant *nse1-C216S* isolated in this study was not sensitive to HU or MMS and suppressed the sensitivity of *smc6-74* to these genotoxic agents; recruitment of mutant Smc5/6 complexes (as assayed by chromatin immunoprecipitation of HA-Nse4) to lesion-containing loci was reduced in the mutant, indicating that dysfunctional Smc5/6 at lesions hinder completion of repair by Smc5/6 independent pathways. These findings indicate an important role for the SpNse1 RING domain in recruitment of Smc5/6 to damaged DNA. In addition to its requirement for resisting DNA damage, SpNse1 is also required for maintenance of checkpoint-induced arrest in response to DNA damage (Harvey et al. 2004) in mitotic cells and proper DNA segregation and homologous recombination during meiosis (Pebernard et al. 2004).

In contrast, relatively little is known about the function of budding yeast Nse1 (henceforth referred to as Nse1 or ScNse1). Nse1 was identified in budding yeast (Fujioka et al. 2002) as an essential nuclear protein associated with the Smc5/6 complex that was likely to have a role in DNA repair. Further studies have demonstrated a role for ScNse1 in Rad52-dependent post replication repair of UV-damaged DNA (Santa Maria et al. 2007). Nse1 has also been shown to be part of a stable trimeric complex consisting of Nse1, 3 and 4 that associates with the Smc5 head region in budding yeast (Duan et al. 2009b). Not much additional information is available regarding the function of ScNse1 at present.

In this study, we investigated the role of the ScNse1 RING domain and found that it is important for interaction with Nse3 and other Smc5/6 complex subunits. Association of Nse1 with other Smc5/6 complex subunits is important for its roles in completion of DNA replication, cohesion and maintenance of chromosome stability.

Materials and methods

Media and reagents

Yeast cells were grown in YPD medium or supplemented minimal medium as indicated. MMS and hydroxyurea (HU) were procured from Sigma, G418 from Calbiochem, hygromycin and nourseothricin from USB, 12CA5 anti-HA antibody and 9E10 anti c-MYC epitope primary antibody from Roche, HRP-conjugated secondary antibodies from Santacruz and Bangalore Genei, and anti-GST antibody was purchased from Bangalore Genei.

Growth and drug sensitivity assays

Yeast cells were grown in selective media to an OD_{600} of 1 and serially diluted tenfold. To assay growth and drug sensitivity, 5 µl of each dilution starting from 10^{-1} was spotted on YPD plates that were incubated at varying temperatures as indicated (23, 30, 34 or 37 °C), or plates having the indicated concentrations of MMS or HU. For analysis of sensitivity to UV radiation, cells were serially diluted and spotted on YPD plates and irradiated with the indicated doses (1500 or 2000 µJ/cm^2) of UV radiation using a UVC-500 cross-linker (Amersham Biosciences). The plates were immediately covered with aluminum foil, incubated at 23 °C for 3–5 days, and images were captured.

Yeast strains, plasmids and oligonucleotides

Yeast strains used in this work are haploids with 'a' mating type. Yeast strains and plasmids used and constructed for this study are listed in Tables 1 and 2, respectively. Oligonucleotides used for this study were synthesized by Sigma Genosys and are listed in Table 3.

Generation of *nse1* mutant yeast strains

An *nse1*Δ*::KanMX6* disruption cassette was created in pSM1 (bearing *NSE1* ORF amplified using SLO10 and SLO453 cloned in pCR™-Blunt II-TOPO® vector) by replacing a SalI–NruI fragment from *NSE1* with *KanMX6* excised from pFA6a-kanMX6 (Bahler et al. 1998) with SalI and EcoRV. The disruption cassette *nse1*Δ*::KanMX6* was amplified from this construct (pSM9) by PCR using gene-specific primers (SLO10 and SLO453) and transformed into W303-1a bearing pSM3. The transformants were selected on G418 (150 µg/ml) containing YPD plates. Plasmid shuffling was carried out by patching on 5-FOA (1 mg/ml) containing

Table 1 Yeast strains used in this study

Strain	Genotype	Source
SLY1632	*MAT*a *leu2-3,112 can1-100 ura3-1 trp1-1 ade2-1 his3-11,15 nse1Δ::KanMX6 (pSM3)*	This study
SLY1651	*MAT*a *leu2-3,112 can1-100 ura3-1 trp1-1 ade2-1 his3-11,15 nse1Δ::KanMX6 (pSM2)*	This study
SLY1652	*MAT*a *leu2-3,112 can1-100 ura3-1 trp1-1 ade2-1 his3-11,15 nse1Δ::KanMX6 (pSM7)*	This study
SLY1653	*MAT*a *leu2-3,112 can1-100 ura3-1 trp1-1 ade2-1 his3-11,15 nse1Δ::KanMX6 (pSM8)*	This study
SLY1884	*MAT*a *leu2-3,112 can1-100 ura3-1 trp1-1 ade2-1 his3-11,15 nse1Δ::KanMX6 (pSM28)*	This study
SLY1885	*MAT*a *leu2-3,112 can1-100 ura3-1 trp1-1 ade2-1 his3-11,15 nse1Δ::KanMX6 (pSM29)*	This study
YYB3476	*MAT*a *bar1Δ ura3-x ade1 leu2-x trp1::TetO:TRP1 lys4::LacO:LEU2 his3::LacR-GFP:HIS3 TetR-mRFP*	Neurohr et al. (2011)
SLY2048	*MAT*a *leu2-3,112 can1-100 ura3-1 trp1-1 ade2-1 his3-11,15 nse1Δ::KanMX6 (pSM48)*	This study
SLY2051	*MAT*a *leu2-3,112 can1-100 ura3-1 trp1-1 ade2-1 his3-11,15 nse1Δ::KanMX6 (pSM49)*	This study
SLY2178	*MAT*a *bar1Δ ura3-x ade1 leu2-x trp1::TetO:TRP1 lys4::LacO:LEU2 his3::LacR-GFP:HIS3 TetR-mRFP nse1Δ::KanMX6* (pSM3)	This study
SLY2213	*MAT*a *leu2-3,112 can1-100 trp1-1 ura3-1 ade2-1 his3-11,15 nse1Δ::KanMX6 (pSM67)*	This study
SLY2214	*MAT*a *leu2-3,112 can1-100 trp1-1 ura3-1 ade2-1 his3-11,15 nse1Δ::KanMX6 (pSM68)*	This study
SLY2246	*MAT*a *leu2-3,112 can1-100 ura3-1 trp1-1 ade2-1 his3-11,15 bar1Δ::LEU2 SCC1 3HA nse1Δ::KanMX6 (pSM2)*	This study
SLY2247	*MAT*a *leu2-3,112 can1-100 ura3-1 trp1-1 ade2-1 his3-11,15 bar1Δ::LEU2 SCC1 3HA nse1Δ::KanMX6 (pSM8)*	This study
SLY2318	*MAT*a *leu2-3,112 can1-100 ura3-1 trp1-1 ade2-1 his3-11,15 SMC5 9MYC:hphNT1 nse1Δ::KanMX6* (pSM3)	This study
SLY2491	*MAT*a *leu2-3,112 can1-100 trp1-1 ura3-1 ade2-1 his3-11,15 SMC5 9MYC:hphNT1 nse1Δ::KanMX6* (pSM67)	This study
SLY2492	*MAT*a *leu2-3,112 can1-100 trp1-1 ura3-1 ade2-1 his3-11,15 SMC5 9MYC:hphNT1 nse1Δ::KanMX6* (pSM68)	This study
SLY2565	*MAT*a *leu2-3,112 can1-100 ura3-1 trp1-1 ade2-1 his3-11,15 SMC5 9MYC:hphNT1 NSE3-3HA:klTRP1 nse1Δ::KanMX6* (pSM65)	This study
SLY2566	*MAT*a *leu2-3,112 can1-100 ura3-1 trp1-1 ade2-1 his3-11,15 SMC5 9MYC:hphNT1 NSE3 3HA:klTRP1 nse1Δ::KanMX6* (pSM66)	This study
SLY2570	*MAT*a *leu2-3,112 can1-100 trp1-1 trp1-1 ade2-1 his3-11,15 his3-11,15 SMC5 9MYC:hphNT1 nse1Δ::KanMX6 NSE3 3HA:klTRP1* (pSM3)	This study
SLY2571	*MATa leu2 trp1 ura3-52 can1 ade2::KAN NSE1:LEU2* /yWSS1572-1	This study
SLY2572	*MATa leu2 trp1 ura3-52 can1 ade2:: KAN nse1-103 :LEU2* /yWSS1572-1	This study
SLY2583	*MATa leu2 trp1 ura3-52 can1 ade2::KAN NSE1:LEU2 /PA3-1*	This study
SLY2584	*MATa leu2 trp1 ura3-52 can1 ade2::KAN nse1-103:LEU2 /PA3-1*	This study
SLY2616	*MAT*a *leu2-3,112 can1-100 ura3-1 trp1-1 ade2-1 his3-11,15 nse1Δ::KanMX6 rrm3Δ::hphNT1 (pSM2)*	This study
SLY2619	*MAT*a *leu2-3,112 can1-100 ura3-1 trp1-1 ade2-1 his3-11,15 nse1Δ::KanMX6 rrm3Δ::hphNT1 (pSM8)*	This study
SLY2628	*MAT*a *leu2-3,112 can1-100 ura3-1 trp1-1 ade2-1 his3-11,15 nse1Δ::KanMX6 rrm3Δ::hphNT1 tof1Δ::natNT2 (pSM2)*	This study
SLY2631	*MAT*a *leu2-3,112 can1-100 ura3-1 trp1-1 ade2-1 his3-11,15 nse1Δ::KanMX6 rrm3Δ::hphNT1 tof1Δ::natNT2 (pSM8)*	This study
SLY2646	*MAT*a *bar1Δ ura3-x ade1 leu2-x trp1::TetO:TRP1 lys4::LacO:LEU2 his3::LacR-GFP:HIS3 TetR-mRFP nse1Δ::KanMX6* (pSM65)	This study
SLY2647	*MAT*a *bar1Δ ura3-x ade1 leu2-x trp1::TetO:TRP1 lys4::LacO:LEU2 his3::LacR-GFP:HIS3 TetR-mRFP nse1Δ::KanMX6* (pSM66)	This study
AH109	MATa, trp1-901, leu2-3, 112, ura3-52, his3-200,gal4Δ, gal80Δ, LYS2 : : $GAL1_{UAS}$–$GAL1_{TATA}$–HIS3,$GAL2_{UAS}$–$GAL2_{TATA}$–ADE2,URA3 : : $MEL1_{UAS}$–$MEL1_{TATA}$–lacZ	Clontech
SLY2246	*MAT*a *leu2-3,112 can1-100 ura3-1 trp1-1 ade2-1 his3-11,15 bar1Δ::LEU2 SCC1 3HA nse1Δ::KanMX6 (pSM2)*	This study
SLY2247	*MAT*a *leu2-3,112 can1-100 ura3-1 trp1-1 ade2-1 his3-11,15 bar1Δ::LEU2 SCC1 3HA nse1Δ::KanMX6 (pSM8)*	This study
SLY2768	*MAT*a *leu2-3,112 can1-100 ura3-1 trp1-1 ade2-1 his3-11,15 bar1Δ::LEU2 SCC1 3HA nse1Δ::KanMX6 (pSM2) mph1::hphNT1*	This study
SLY2769	*MAT*a *leu2-3,112 can1-100 ura3-1 trp1-1 ade2-1 his3-11,15 bar1Δ::LEU2 SCC1 3HA nse1Δ::KanMX6 (pSM8) mph1::hphNT1*	This study

Table 2 Plasmids used in this study

Plasmid	Brief description	Source/ref.
pSM1	pCR™-Blunt II-TOPO®-*NSE1*	This study
pSM2	pRS314 bearing *NSE1* in EcoRI-site	This study
pSM3	pRS316 bearing *NSE1* in EcoRI-site	This study
pSM7	pRS314 bearing *nse1-101* in EcoRI site	This study
pSM8	pRS314 bearing *nse1-103* in EcoRI site	This study
pSM9	PCR TOPOII bearing *nse1Δ::KANMX6* in SalI-/NruI-site	This study
pSM28	pRS314 bearing *nse1-104* in SmaI-site	This study
pSM29	pRS314 bearing *nse1-105* in SmaI-site	This study
pGBKT7	Matchmaker Two-Hybrid System 3 vector for fusion of Gal4-DNA binding domain and c-MYC epitope to bait protein (markers: *TRP1*, kanamycin^R)	Clontech
pGADT7	Matchmaker Two-Hybrid System 3 vector for fusion of Gal4-AD (Activation Domain) and HA epitope to test protein (markers: *LEU2*, ampicillin^R)	Clontech
pDB30	pGBKT7 bearing *NSE4* in EcoRI–BamHI site	This study
pSM37	pGADT7 bearing *NSE1* in EcoR1–BamHI site	This study
pSM74	pGADT7 bearing nse1-103 in EcoR1–BamHI site	This study
pSM41	pGBK-T7 bearing *NSE1* in EcoRI–BamHI site	This study
pDS58	pGADT7 bearing *NSE3* in EcoRI–BamHI site	This study
pDS72	pGEX-4T-1 bearing *NSE3* in BamHI–EcoR1 site	This study
pGEX-4T-1	Parent plasmid for creating GST-fusion constructs	Kaelin et al. (1992)
pSM45	plasmid bearing 350 bp downstream of *NSE1* in EcoR1–Sma1 sites of pUC19	This study
pSM48	pAML10/HA-*NSE1* bearing *NSE1* in BamHI-/PstI-site	This study
pSM49	pAML10/HA-*NSE1* derived plasmid having *nse1-103* replacing *NSE1* in BamHI-/PstI-site	This study
pSM65	pRS412 bearing *NSE1*	This study
pSM66	pRS412 bearing *nse1-103*	This study
pSM67	pRS423-GPD bearing *3HA NSE1* in BamHI-/PstI-site	This study
pSM68	pRS423-GPD bearing *3HA nse1-103* in BamHI-/PstI-site	This study
pSM69	pGBKT-7 bearing *nse1-103* in BamHI-/EcoRI-site	This study
pSM71	pSM45 having *nse1-103* ORF in BamH1–HincII sites	This study
pSM72	pUC19 bearing *nse1-103:LEU2*	This study
pSM73	pUC19 bearing *NSE1:LEU2*	This study
pSM75	pSM45 having *NSE1* in BamH1–HincII sites	This study
pYM16	Plasmid having 6HA epitope tag and *hphNT1*	Janke et al. (2004)
pYM17	Plasmid having 6HA epitope tag and *natNT2*	Janke et al. (2004)
pYM20	Plasmid having 9Myc epitope tag and *hphNT1*	Janke et al. (2004)
pYM22	plasmid having 3HA epitope tag and *klTRP1*	Janke et al. (2004)
pAML10/HA-NSE1	pAML10 (*LEU2*, CEN vector having *ADH1*-promoter driving *HA-NSE1* that expresses a fusion protein that has 3 copies of the HA-epitope fused to the N-terminal end of Nse1	Fujioka et al. (2002)

synthetic complete (SC) plates. Transformants that failed to grow on 5-FOA plates were further screened by colony PCR using primers SLO124 and SLO480 that produce a fragment of 593 bp, in case of integration of the *nse1* knockout cassette at the correct endogenous locus, to identify the desired strain SLY1632.

Site-directed mutagenesis was performed by overlapping PCR using two mutagenic primers [C289A: SLO457/SLO456; H306A: SLO575/SLO574; C309A: SLO577/SLO576; H306A C309A: SLO459/SLO458; C289A H306A C309A was created using pSM8 (a plasmid having *nse1-103* cloned in pRS314) as the template and SLO457/SLO456 as the mutagenic primers] in combination with two flanking primers (SLO10 and SLO453). Two PCR reactions were performed using one normal and one mutagenic primer. The two PCR fragments were pooled and used as a template for the final PCR reaction using the flanking primers (SLO10 and SLO453). The PCR product thus obtained was ligated to pCR™-Blunt II-TOPO® vector and the constructs obtained were verified by restriction digestion with EcoR1 and sequencing. The fragments bearing mutations were excised with EcoR1 and ligated to EcoRI-cut pRS314.

Table 3 Oligonucleotide primers used in this study

Name	Sequence
SLO6	5′TCTTCTGGTCTGTATCTTCT3′
SLO10	5′AATGCTCCTCTTTTCTGCGT3′
SLO124	5′CGCTATACTGCTGTCGATTC3′
SLO311	5′ AGGATCCGAAGATGATACATTTCGGTGAAACTTCTAACTACTCATTCGATCGT ACGCTGCAGGTCGAC 3′
SLO312	5′ AAACATGTTTACATCTATATGTGTATAATTAATTATGCAATAGTGAAAGA TTAATCGATGAATTCGAGCTC G 3′
SLO444	5′TAGTAACCCGTTTAAGTCCAGTC3′
SLO453	5′TCAATCACATGCCGTTTAG3′
SLO456	5′GCAACGAATCAGCCCGAGAAGAGAAT3′
SLO457	5′CATTCTCTTCTCGGGCTGATTCGTTGC3′
SLO458	5′CAAATTTGGGCTGTTGATGCTTTCAAGCATT3′
SLO459	5′GCTTGAAAGCATCAACAGCCCAAATTTGA3′
SLO480	5′TATAAACCTCGAACCGTG3′
SLO484	5′GGCGGATCCATGAGTTCTATAGATAAT3′
SLO485	5′GGCGAATTCCTATATAGAATATGAATCG3′
SLO536	5′ ATGGAGGTACATGAAGAG3′
SLO574	5′CAAATTTGGGCTGTTGATTGTTTCAAGCATT3′
SLO575	5′GCTTGAAACAATCAACAGCCCAAATTTGA3′
SLO576	5′CAAATTTGGCATGTTGATGCTTTCAAGCATT3′
SLO577	5′GCTTGAAAGCATCAACATGCCAAATTTGA3′
SLO631	5′TAGCAGAATTCATGGAGGTACATGAAGAG3′
SLO632	5′TCAGAGGATCCTTAAATAACGTATACGCC3′
SLO643	5′TACAATCAACTCCAAGCTGAC3′
SLO644	5′TGGATCGGGCTGTAGGGAGGTACATGAAG3′
SLO645	5′ATGTACCTCCCTACAGCCCGATCCAG3′
SLO646	5′TGCTGCAGTTAAATAACGTATACGCCCTC3′
SLO651	5′ACTAAAATAC ATAGCTTTCC3′
SLO652	5′ACTACTGCCTTCTTGAAAGGC3′
SLO791	5′CGAGCTCGAATTCATCGAT3′
SLO834	5′ACTAAAAGTTTGCACGATGATATAATAAAAAGCATTGGCGATTCATATTCTATACGTACGCTGCAGGTCGAC 3′
SLO835	5′ATTTCCTCGACAAAAAAGATGCGCACCTAAACTACATGGACACCTATGCAATGCTAATCGATGAATTCGAGCTCG 3′
SLO836	5′AAGCAGAGGAGAACAAGCTCAAAAGTCGAGAGATTTGTTCTTATAAGACATCCCGCGTACGCTGCAGGTCGAC3′
SLO837	5′AGAACAAGAAAAGAAAACTTCAACTAGAGTATATGCATTTATTCG TTGCAAGTCAATCGATGAATTCGAGCTCG3′
SLO838	5′AATACCATCTAGCTTGTGGGGTTTAGTGTATCTTTAATATAGGAGGG CGCACACTCGTACGCTGCAGGTCGAC3′
SLO839	5′AGTGGTTCTAAAATTACACGTATTAAAGGGATTAATTACTACATATTC ATTCTCAATCGATGAATTCGAGCTCG3′
SLO840	5′TACGTAGGCTTAGCTAAATAG3′
SLO841	5′TCCTAATGGACATTTGAGTTC3′
SLO890	5′GGCGAATTCATGTCTAGTACAGT3′
SLO891	5′CGAGGATCCTTAGTCTAAGAATG3′
SLO918	5′ATTCAACACATTCCGGTTCTGTTTTATTTTAGTGTCCTTTTTTCTCTCTGATGCGTACGCTGCAGGTCGAC3′
SLO919	5′ATTACAGCAGCGTTATTTTTGTATAGACGCCGACGTATAAGAGTCTCCTATCAATCGATGAATTCGAGCTCG3′
SLO920	5′ CCGTATCCTTAATGAATG 3′

Creation of replication factor defective mutants *rrm3Δ*, *tof1Δ* and *mph1Δ*

The *rrm3, tof1* and *mph1* deletion mutants were created by one-step PCR-mediated gene disruption. The disruption cassette *rrm3Δ::hphNT1* was amplified from pYM16 (Janke et al. 2004) using the primer pairs SLO836/SLO837, transfected into yeast cells and transformants were selected using 300 µg/ml hygromycin. The correct insertion was further verified by PCR using the primers SLO791 and SLO840

that produces a fragment of 145 bp upon correct integration. The *tof1Δ::natNT2* disruption was created using the primers SLO838 and SLO839, and pYM17 (Janke et al. 2004), as the template to amplify the disruption cassette by PCR. Transformants were selected using 100 µg/ml nourseothricin and correct integration verified by PCR using SLO791 and SLO841 that generates a 180-bp fragment in desired integrants. *MPH1* was disrupted by the *hphNT1* marker using primers SLO918/SLO919 to PCR amplify a disruption cassette from pYM16. The PCR product was transformed into yeast and colonies were selected on YPD plates containing hygromycin (300 µg/ml). Correct integration at the *MPH1* locus was confirmed by colony PCR using primers SLO920 and SLO791 that produce a fragment of 158 bps in desired integrants.

Plasmid construction

The plasmids expressing 3HA-tagged versions of *NSE1* or *nse1-103* were made as follows: A 165-bp fragment having 3HA fused to part of *NSE1* was amplified from pAML10/*HA NSE1* (Fujioka et al. 2002) using primers SLO643 and SLO645. A 1022-bp fragment was amplified from pSM2 or pSM8 using the primers SLO644 and SLO646. The two fragments (165 bp and 1022 bp) were pooled and used as a template for PCR with flanking primers SLO643 and SLO646 to give a 1.2 kb PCR fragment that was cut with BamHI–PstI and ligated to BamHI–PstI-cut pAML10/HA-*NSE1* to give pSM48 (3HA-*NSE1*) and pSM49 (3HA-*nse1-103*), respectively. To generate 2-µ variants of the above, pSM48 or pSM49 were cut with BamHI-PstI and ligated to BamHI–PstI-cut pRS423-GPD to create pSM67 and pSM68, respectively.

The plasmids pSM73 and pSM72 bearing the *NSE1:LEU2* or *nse1-103:LEU2* integration cassettes were constructed as follows: 395 bp downstream of *NSE1* was amplified from W303-1a genomic DNA using primers SLO651 and SLO652 using Phusion polymerase (NEB). The fragment was digested by EcoRI to get a 352-bp fragment that was ligated to EcoRI–SmaI cut pUC19, generating pSM45. *NSE1*/*nse1-103* ORFs were amplified from pSM2/pSM8 using primers SLO536 and SLO632. The 1.1 kb fragments obtained were cut with BamHI and ligated to BamHI-HincII-cut pSM45 to generate pSM75 and pSM71, respectively. *LEU2* was excised (from pRR70) with BglII and ligated to BamHI-cut pSM75/pSM71, generating pSM73/pSM72.

Yeast two hybrid assay

Protein–protein interaction was determined by the yeast two-hybrid assay using the reporter strain AH109. The plasmids pGBKT7 and pGADT7 bearing Gal4-BD or Gal4-AD, respectively, served as vector backbones for cloning *NSE1* (using primers SLO631/632), and its variants, *NSE3* or *NSE4*, (using primers SLO890/891) to produce the respective fusions using standard methods. Combinations of the test plasmids were transformed into AH109 and transformants were selected on SC plates lacking leucine and tryptophan. For testing the interaction between proteins, the cells were spotted on SC plates lacking leucine, tryptophan and histidine with or without 3-Amino Triazole (3-AT) after normalizing the OD_{600}.

Cloning, expression and purification of GST-Nse3

A GST–Nse3 fusion protein expressing plasmid pDS72 was constructed by cloning *NSE3* (PCR amplified using primers SLO484 and SLO485) into BamHI–EcoR1-cut pGEX4T1 (Kaelin et al. 1992). The construct was verified by sequencing and transformed into the bacterial expression strain BL21(DE3). Cells at OD_{600} of ~0.5 were induced by adding 0.3 mM IPTG and grown at 16 °C for 10 h. For the affinity purification, cells from 1 L culture were pelleted and resuspended in 20 ml of PBS lysis buffer (150 mM NaCl, 20 mM sodium phosphate buffer pH 7.4, 1% tritonX-100) with protease inhibitors (1 µg/ml leupeptin, 25 µg/ml PMSF) and sonicated for 10 cycles (1sec on and 3sec off) on ice, centrifuged at 12,500 rpm for 30 min (4 °C). The supernatant was added to 5 ml of glutathione Sepharose beads equilibrated in PBS lysis buffer and incubated on a nutator (8 rpm, 6–8 h in the cold room). Samples were centrifuged at 1500 rpm for 2 min at 4 °C. The beads were washed thrice with ice-cold PBS (150 mM NaCl, 20 mM sodium phosphate buffer pH 7.4) having protease inhibitors. The fusion protein was eluted by adding 5 ml of ice-cold 50 mM Tris–Cl (pH 8) containing 20 mM reduced glutathione.

GST pull-down assay

Yeast strains expressing epitope-tagged Nse1-3HA or nse1-103-3HA were created by transforming pSM67 or pSM68 into SLY1632 followed by plasmid shuffling on 5-FOA (1 mg/ml) plates.

Yeast cell lysate was prepared as mentioned in (Pfander et al. 2005). Briefly, yeast native extract was prepared by glass bead lysis in 150 mM NaCl, 50 mM Tris–HCl pH 7.4 (20 cycles of vortexing for 1 min) on ice, followed by detergent extraction (1% Triton X-100, 0.05% SDS) and precleared by centrifugation (12,500 rpm for 30 min at 4 °C). For the pull-down assay, 50 mg of GST or GST–Nse3 fusion protein bound to beads was incubated with 2.5 mg of yeast native lysate overnight at 4 °C. Beads were then washed and eluted in sample buffer containing 8 M urea. Whole-cell extract samples correspond to 1/10 of the total input.

Co-immunoprecipitation of proteins

Yeast strains co-expressing Smc5-9Myc and Nse1-3HA or Nse3-3HA were created as follows. SLY1632 was transformed with *SMC5 9MYC:hphNT1* PCR fragment, amplified using primers SLO311 and SLO312, and pYM20 (Janke et al. 2004) as a template. The transformants were selected on YPD plates containing hygromycin (300 µg/ml). Screening for the epitope tagging of SMC5 was done by colony PCR using SLO6 and SLO791 as primers, which should give a fragment of size 540 bp in the desired strain, SLY2318. SLY2318 was transformed with pSM67 (a 2-µ plasmid expressing *3HA-NSE1*) and selected on SC–ura–his plates; pSM3 was shuffled out on SC plates containing 5-FOA (1 mg/ml) to obtain SLY2491. To obtain the strain co-expressing Smc5-9Myc and nse1-103-3HA (a 2-µ plasmid expressing *3HA-nse1-103*), SLY2318 was transformed with pSM68 and selected on SC–ura–his plates; pSM3 was shuffled out on SC plates containing 5-FOA (1 mg/ml) to obtain SLY2492. To epitope-tag Nse3, *NSE3 3HA :klTRP1* PCR fragment, amplified using oligos SLO834 and SLO835 with pYM22 (Janke et al. 2004) as template was transformed into SLY2318. The transformants were selected on SC–Ura–Trp plates and screened by colony PCR using primers SLO444 and SLO791 that give a fragment of size 144 bp in the desired strain SLY2570. SLY2570 was transformed with pSM65 or pSM66 and selected on SC–Ade. Transformants were patched on SC plates containing 5-FOA (1 mg/ml) for plasmid shuffling to obtain the wild-type and *nse1-103* strains SLY2565 and SLY2566, respectively.

Protein lysate was prepared as described in (Bustard et al. 2016). Cells expressing Myc-tagged Smc5 were grown at 25 °C to log phase, pelleted and resuspended in 500 µl lysis buffer (50 mM HEPES pH 7.5, 140 mM NaCl, 1 mM EDTA, and 1% Triton X-100). Equal volume of glass beads was added and cells were lysed for a total of 20 cycles (1 cycle–1 min on vortexer and 1 min on ice), followed by centrifugation at 12,500 rpm for 30 min at 4 °C. Supernatant was collected and kept on ice. About 1 mg of protein was incubated overnight with 0.4 µg 9E10 anti-MYC antibody on a nutator (4 °C). Protein G-Sepharose (30 µl) washed twice with lysis buffer were added to the protein–Ab mixture and incubated at 4 °C for 3–4 h. Beads were spun down (2000 rpm, 4 °C for 2 min) and washed once in lysis buffer and twice in wash buffer (100 mM Tris (pH 8), 0.5% Nonidet P-40, 1 mM EDTA and 300 mM NaCl). The last wash was done in wash buffer containing 1M NaCl[100 mM Tris (pH 8), 0.5% Nonidet P-40, 1 mM EDTA and 1M NaCl]. Beads were resuspended in 2x Laemmli buffer, boiled for 10 min and centrifuged (12,500 rpm for 15 min, RT) and the supernatant was run on a 8% SDS–polyacrylamide gel, followed by Western blotting using anti-HA (12CA5) and anti-MYC (9E10) antibodies.

Immunodetection of proteins

Protein extracts were prepared from yeast as described in (Kushnirov 2000). Briefly, about 2.5 OD_{600} yeast cells were harvested by centrifugation from liquid culture. The cells were resuspended in 100 µl distilled water, to which 100 µl 0.2M NaOH was added, and then incubated for 5 min at room temperature, pelleted, and resuspended in 50 µl SDS sample buffer (0.06 M TrisHCl, pH 6.8, 5% glycerol, 2% SDS, 4% β-mercaptoethanol, 0.0025% bromophenol blue). The samples were boiled for 3 min and centrifuged again. The samples were run on 10% SDS PAGE, transferred to a nitrocellulose membrane (from GE-Healthcare) and probed using anti-HA (12CA5) primary antibody (1:5000 dilution) and HRP-conjugated goat anti-mouse secondary antibody (1:5000 dilution). ECL reagents from Perkin Elmer were used for detection.

Gross chromosome rearrangement (GCR) assay

Strains for measuring GCR frequency were created by integrating the *NSE1:LEU2* or *nse1-103:LEU2* in the strains DH1003/102 and DH2004-1/101 containing either the smaller (yWSS1572-1) or larger (PA3-1) YACs, respectively (Huang and Koshland 2003). The primers SLO536 and SLO453 were used to amplify *NSE1:LEU2* or *nse1-103:LEU2* from pSM73 and pSM72, respectively. For the GCR assay, the strains were plated on SC–ura plates and single colonies were picked and resuspended in 1 ml of sterile water. The samples were diluted such that ~200 colonies would be produced on each YPD plate after plating. After growth at 23 °C, the colonies were replica-plated on SC–Trp and SC–Ura plates to estimate the telomere marker loss (Trp^+, Ura^-) or whole YAC loss (Trp^-, Ura^-). Nearly 2000 colonies were counted for each experiment.

Cohesion assay

For assaying cohesion, wild-type or *nse1-103* cells (SLY2646 and SLY2647) (2 ml of log phase culture of OD_{600} ~ 0.6) were arrested in the G2/M phase of the cell cycle by adding nocodazole (15 µg/ml) and incubating for 2 h. To prepare samples for confocal microscopy, cells were spun down, vortexed after adding 100 µl of paraformaldehyde and incubated for 15 min at room temperature in the dark. The supernatant was removed and cells were washed once in 1 ml of KPO_4/sorbitol (0.1M potassium phosphate, 1.2M sorbitol). The cells were resuspended in a small volume (~200 µl) of KPO_4/sorbitol solution and stored at 4 °C. Before performing microscopy, cells were sonicated gently (7 bursts, 10% Duty cycle, output control 1) and 3 µl cells were put on an agarose-coated glass slide. Images were captured using Zeiss LSM 880 confocal microscope (0.6

micron sections). Images were analyzed using Zen Black 2.1 software and cohesion events in nearly 100 nuclei were enumerated for each sample.

Construction of strains used for the cohesion assay

The strain YYB3476 having a LacO array on the left arm of ChrIV at *lys4* and expressing lacI–GFP (Neurohr et al. 2011), and also harboring the plasmid pSM3 (pRS316-*NSE1*), was transformed with a disruption cassette *nse1Δ::KanMX6* that was amplified from pSM9 by PCR-using gene-specific primers (SLO10 and SLO453) and transformants were selected on G418 (150 µg/ml) containing YPD plates. Transformants which did not grow on 5-FOA plates were further screened by colony PCR using primers SLO124 and SLO480 to produce a 593-bp PCR fragment confirming *nse1* disruption at the correct endogenous locus. The strain thus generated, SLY2178, was transformed with pSM65 (pRS412–*NSE1*) or pSM66 (pRS412–*nse1-103*) and transformants selected on SC–Ade plates. The transformants were then patched on 5-FOA–SC plates to generate *NSE1* (SLY2646) or *nse1-103* (SLY2647) strains lacking pSM3.

Pulsed-field gel electrophoresis (PFGE)

A 0.8% agarose gel (PFGE-grade agarose from Biorad) in 0.5X TBE was cast and chromosomal DNA plugs were placed in the wells and sealed by pouring 0.8% agarose over it. The gel was run in 0.5X TBE with a switch time ramped from 60 to 120 s, 3.5 V/cm, for 24 h using the Biorad CHEF-DR III system. The chromosomes were stained by ethidium bromide (0.5 µg/ml) post-run.

Chromosomal DNA plugs for PFGE were prepared as described previously (Iadonato and Gnirke 1996) and summarized below. The wild-type or the mutant cells were grown overnight and subcultured to an OD_{600} of 0.1. Cells were grown to an OD_{600} of ~0.3 and arrested in G1 by adding α-mating pheromone (50 ng/ml) to YPD medium and grown for 2–3 h. G1-arrested cells were observed under the microscope and also by FACS. Cells were then washed twice with water and grown in YPD at the indicated temperature. Cells were harvested at different time points by centrifugation at 3000 rpm for 5 min and washed twice with 50 mM EDTA. The cells were resuspended in 50 mM EDTA to a final concentration of 2×10^9 cells/ml and kept at 45 °C for 5 min. Equal volume of 2% agarose (PFGE-grade agarose from Bio-rad) in 50 mM EDTA also prewarmed to 45 °C was added to the cell suspension and mixed with a pipette. Almost 70 µl of each sample was aliquoted into each plug mold to harden (at 4 °C for 15 min.). Plugs of the same sample were extruded from the plug mold into a six-well dish. To each well, 3 ml of freshly prepared spheroplasting solution (1 M Sorbitol, 20 mM EDTA (pH 8.0), 10 mM Tris–HCl (pH7.5), 14 mM 2-mercaptoethanol, 0.5 mg/ml zymolase 20-T) was added and the samples were incubated at 37 °C for 4–6 h with gentle shaking (40 rpm). The spheroplasting solution was aspirated off and 2–3 ml of LDS solution (1% lithium dodecyl sulfate, 100 mM EDTA, 10 mM Tris–HCl, pH 8.0) was added followed by incubation with gentle shaking at 37 °C for at least 15 min. After removal of the LDS solution, fresh LDS solution was added and incubated with gentle shaking at 37 °C for 8–10 h. The plugs were washed thrice (30 min each) 3 ml of 0.2x NDS solution (0.5M EDTA, 10 mM Tris base, 1% sarkosyl (pH 9.5)) with gentle shaking at room temperature followed by 3 ml of TE (five times, 30 min each), pH 8.0, with gentle shaking at room temperature. The plugs were stored at 4 °C in six-well dishes with TE, pH 8.0, covered with Saran wrap to prevent excessive evaporation.

Bioinformatic analysis

Multiple sequence alignment was performed by aligning the RING-domains of Nse1-related proteins with ClustalW using default parameters. The sequences of the Nse1 orthologs included in the alignment shown in Fig. 1 are from: *Saccharomyces cerevisiae* (S.c.)(aa 271-324, accession number KZV09254), *Homo sapiens* (H.s.)(aa 182-227, AAH18938), *Drosophila melanogaster* (D.m.)(aa 181-224, NP_001260145), *Arabidopsis thaliana* (A.t.)(aa 198-240, AAS92326), *Danio rerio* (D.r.)(aa 153-200, AAH76252), *Xenopus laevis* (X.l.)(aa 182-227, AAH60339), *Mus musculus* (M.m.)(aa 202-247, AAH31848), *Rattus norvegicus* (R.n.)(aa 215-256, AAH99757), *Bos taurus* (B.t.)(aa 178-223, AAI02215), *Aspergillus fumigates* (A.f.)(aa 239-281, KMK58621), *Schizosaccharomyces pombe* (S.p.)(aa 181-221, CAI84978).

Homology modeling of budding yeast Nse1–Nse3 heterodimer was performed using the Swiss-model server (https://swissmodel.expasy.org/) Heteroproject BETA (Arnold et al. 2006; Benkert et al. 2011; Biasini et al. 2014; Guex et al. 2009; Kiefer et al. 2009) using the structure of human NSE1–MAGEG1 (3NW0) (Doyle et al. 2010) as the template.

Results

The Nse1 RING-domain H306 and C309 are important for resisting extrinsic genotoxic stress

Nse1 has a highly conserved C-terminal RING domain that is a cysteine-rich sequence motif that forms a cross brace structure coordinating two Zn^{2+} ions (Borden and Freemont 1996; Pickart 2001). Comparison of the amino acid sequence of the *S. cerevisiae* Nse1 RING domain with that

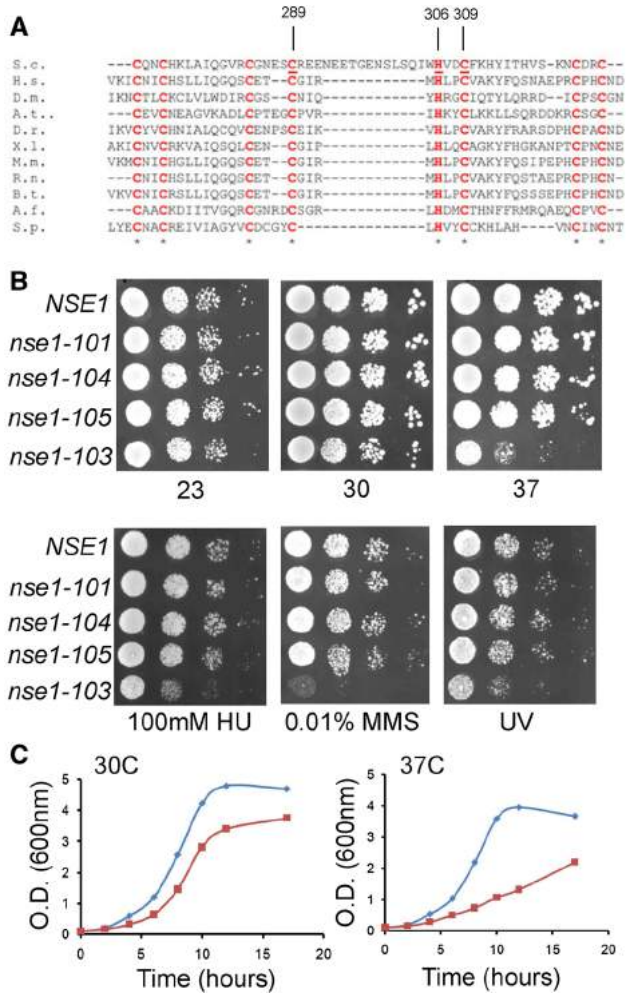

Fig. 1 Characterization of growth properties of RING-domain-targeted mutants of *NSE1*. **a** Multiple sequence alignment of the RING-domain of Nse1-related proteins. Identical conserved residues (depicted in red) of *S. cerevisiae* Nse1 (Cys-289, His-306 and Cys-309) that were mutated to alanine in this study are underlined. "*" denotes identical residues (100% identity) also denoted by red font. The sequences included are *Saccharomyces cerevisiae* (S.c.), *Homo sapiens* (H.s.), *Drosophila melanogaster* (D.m.), *Arabidopsis thaliana* (A.t.), *Danio rerio* (D.r.), *Xenopus laevis* (X.l.), *Mus musculus* (M.m.), *Rattus norvegicus* (R.n.), *Bos taurus* (B.t.), *Aspergillus fumigates* (A.f.), *Schizosaccharomyces pombe* (S.p.). **b** Growth defect and assessment of sensitivity of *nse1* mutants to DNA damage induction. To confirm the sensitivity of the *nse1* mutant cells to extrinsic genotoxic stress, WT (wild-type) and various *nse1* mutant strains [WT (SLY1651); C289A, *nse1-101*(SLY1652); H306A, *nse1-104* (SLY1884), C309A, *nse1-105* (SLY1885), and H306A C309A, *nse1-103* (SLY1653)] were grown to mid-log phase, serially diluted (10-fold), spotted onto YPD at 23, 30 or 37 °C to determine temperature sensitivity (*top* panels) or on YPD plates containing HU (100 mM), MMS (0.01%) or subjected to UV irradiation (2000 μJ/cm^2) at 23 °C and incubated for 3–4 days. **c** The graph depicts the slow growth of *nse1-103* mutant cells (red squares) (SLY1653) relative to wild-type cells (blue diamonds) (SLY1651) in liquid medium at 30 and 37 °C

of the Nse1 protein in fission yeast (*S.p.*), humans (*H.s.*) and other organisms revealed the presence of seven conserved Cysteines and one conserved Histidine residue (Fig. 1a). To investigate the function of the RING domain of Nse1, we created site-specific substitution mutations in the conserved metal-binding cysteine or histidine residues of this domain. We first created a substitution mutation taking a clue from fission yeast in which a mutation in C199 was shown to be defective under various stress conditions (Pebernard et al. 2008). Surprisingly, a corresponding C289A mutation in budding yeast Nse1 *(nse1-101)* did not show any significant defect compared to the wild-type upon exposure to high temperature, HU, MMS or UV (Fig. 1b). We then mutated H306 and/or C309 to alanine and observed that the single mutants, i.e., *nse1H306A (nse1-104)* or *nse1C309A (nse1-105)* showed no growth defect but the double point mutant, i.e., *nse1H306A C309A(nse1-103)*, shows a strong growth defect phenotype (Fig. 1b). The *nse1-103* mutant displayed mild slow growth at 23 and 30 °C and was very slow growing at 37 °C on plates (Fig. 1b, top panels) as well as in liquid media (Fig. 1c). In addition, *nse1-103* is sensitive to genotoxic agents, such as hydroxyurea (HU), methyl methane sulfonate (MMS), and ultraviolet radiation (UV) (Fig. 1b, bottom panels). Hence, *nse1-103* was used for further studies.

We compared the steady-state level of the nse1-103 protein with wild-type by epitope tagging the Nse1 protein with the 3HA-epitope followed by western blotting of yeast cell lysates resolved by SDS–PAGE. The steady-state level of the mutant protein was comparable to wild-type (Fig. S1b), although occasionally, we observed slight reduction of the mutant protein relative to wild-type Nse1 (not shown) in cell extracts. To confirm that the phenotype is not merely a consequence of reduction in level of the mutant protein, we over-expressed both nse1-103 and Nse1 proteins using the 2-μ plasmid and found that the *nse1-103* mutant still exhibited the defective phenotypes (particularly to genotoxic agents) (Fig S1a, bottom two rows) even when the mutant nse1-103 protein was over-expressed (Fig S1b), indicating that the defective phenotypes arise from a defect in protein function rather than its mildly reduced availability.

The nse1-103 mutant protein is defective in interaction with Nse3 and other subunits of the Smc5/6 complex

Nse1, Nse3 and Nse4 associate to form a trimeric sub-complex associated with the ATP-binding head domains of Smc5 and Smc6 proteins within the Smc5/6 complex (Palecek et al. 2006). We employed the yeast two-hybrid assay to test whether the RING-domain mutant protein, nse1-103 could associate with Nse3 and Nse4, its partners within the trimeric sub-complex. The interaction between Nse1 and Nse3, the MAGE-related partner protein could

indeed be demonstrated by the yeast two-hybrid assay when Nse1 fused to the Gal4 DNA binding domain and Nse3 fused to the activation domain were expressed in the yeast strain AH109 having *HIS3* as the reporter gene (Fig. 2a), as expected. However, the nse1-103 protein appeared to be defective in interaction with Nse3 on histidine omission selective plates having 1 mM or higher concentrations of 3-amino triazole (3-AT) (Fig. 2a).

The Nse1/3 RING–MAGE complex also interacts with Nse4 and the head domain of Smc5 within the Smc5/6 complex. Hence, we determined the state of association of the nse1-103 mutant protein with these other subunits. Using the yeast two-hybrid assay in which Nse1 or nse1-103 fused to the Gal4-activation domain were co-expressed with Nse4 fused to the Gal4 DNA binding domain, we found that nse1-103 was also defective in interaction with Nse4, the kleisin partner subunit (Fig. 2b).

We also verified the interaction defect between Nse3 and nse1-103 by a physical assay. GST–Nse3 bound to Glutathione Sepharose beads was able to specifically and efficiently enrich for Nse1-3HA but not nse1-103-3HA from wild-type or mutant yeast extracts, respectively. (Fig. 3a, top panel), further confirming the result obtained by the yeast two-hybrid assay.

In addition, by co-immunoprecipitation of 3HA-tagged Nse1 or nse1-103, with 9Myc-tagged Smc5 from yeast cell extracts, we found that the binding of nse1-103 to Smc5 was drastically reduced (Fig. 3b). Interestingly, the association of Smc5-9Myc with Nse3-3HA appeared to be unaltered in the *nse1-103* mutant relative to wild-type cells (Fig. 3c), indicating a preservation of interactions between the other subunits of the complex in the *nse1-103* mutant.

Enhanced chromosome loss in *nse1-103* mutant cells

To test the effect of the nse1-103 RING domain mutations on the maintenance of chromosomal stability, we used a genetic assay (Huang and Koshland 2003) to score for GCRs (Gross Chromosomal Rearrangements). This assay utilizes extremely telocentric YACs with a short arm of 6 kb and a long arm of 1600 kb (PA3-1) or 332 kb (yWSS1572-1) having selectable markers *URA3* and *ADE2* near the telomere (Fig. 4a). The YACs being dispensable for the growth of cells, allow detection and quantification of chromosomal aberrations occurring within haploid yeast cells. Loss of telomere proximal markers *URA3* and *ADE2* coupled with retention of *TRP1*, the centromere proximal marker on the short arm, represents a chromosome breakage event whereas loss of the centromere proximal marker *TRP1* as well as the telomeric markers represents a chromosomal loss event. To test the requirement of Nse1 for maintenance of chromosome stability, we derived strains having the *nse1-103* mutant allele that also harbor one of the two YACs, PA3-1 or

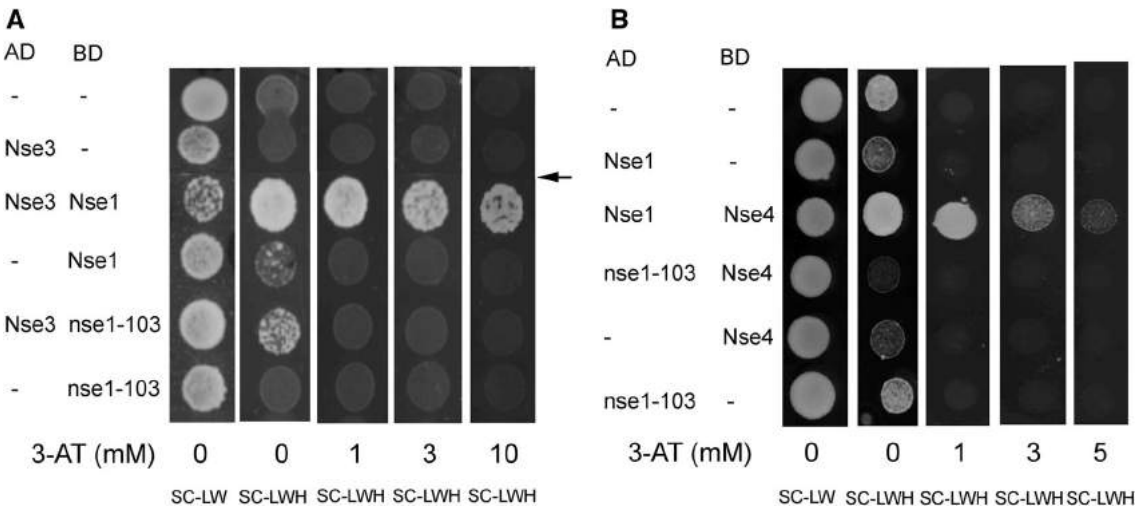

Fig. 2 Determination of interaction of wild-type and mutant Nse1 proteins with other trimeric complex subunits by the yeast two-hybrid assay. **a** The nse1-103 mutant protein is defective in interaction with Nse3. Transformants of strain AH109 bearing the plasmids pGBKT7 (BD), pGADT7 (AD) and their derivatives pGBKT7-*NSE1*(pSM41), pGBKT7-*nse1-103*(pSM69) and pGADT7-*NSE3* (pDS58) were resuspended and after normalizing the OD_{600} were spotted on synthetic complete plates lacking leucine, tryptophan or histidine (SC-LW, SC-LWH or SC-LWH with varying concentrations of 3-AT) as indicated. The arrow indicates site of juxtaposition of ROI (region of interest) of images of spots of different regions from the same plate. **b** Interaction defect of nse1-103 with Nse4. Transformants of strain AH109 bearing the plasmids pGBKT7 (BD), pGADT7 (AD) and their derivatives pGBKT7-*NSE4*(pDB30), pGADT7-*NSE1*(pSM37) and pGADT7-*nse1-103* (pSM74) were resuspended and after normalizing the OD_{600} were spotted on the indicated synthetic complete plates lacking leucine, tryptophan or histidine (SC-LW, SC-LWH or SC-LWH with varying concentrations of 3-AT). Growth on the triple selection plates SC-LWH containing 3-AT indicates interaction

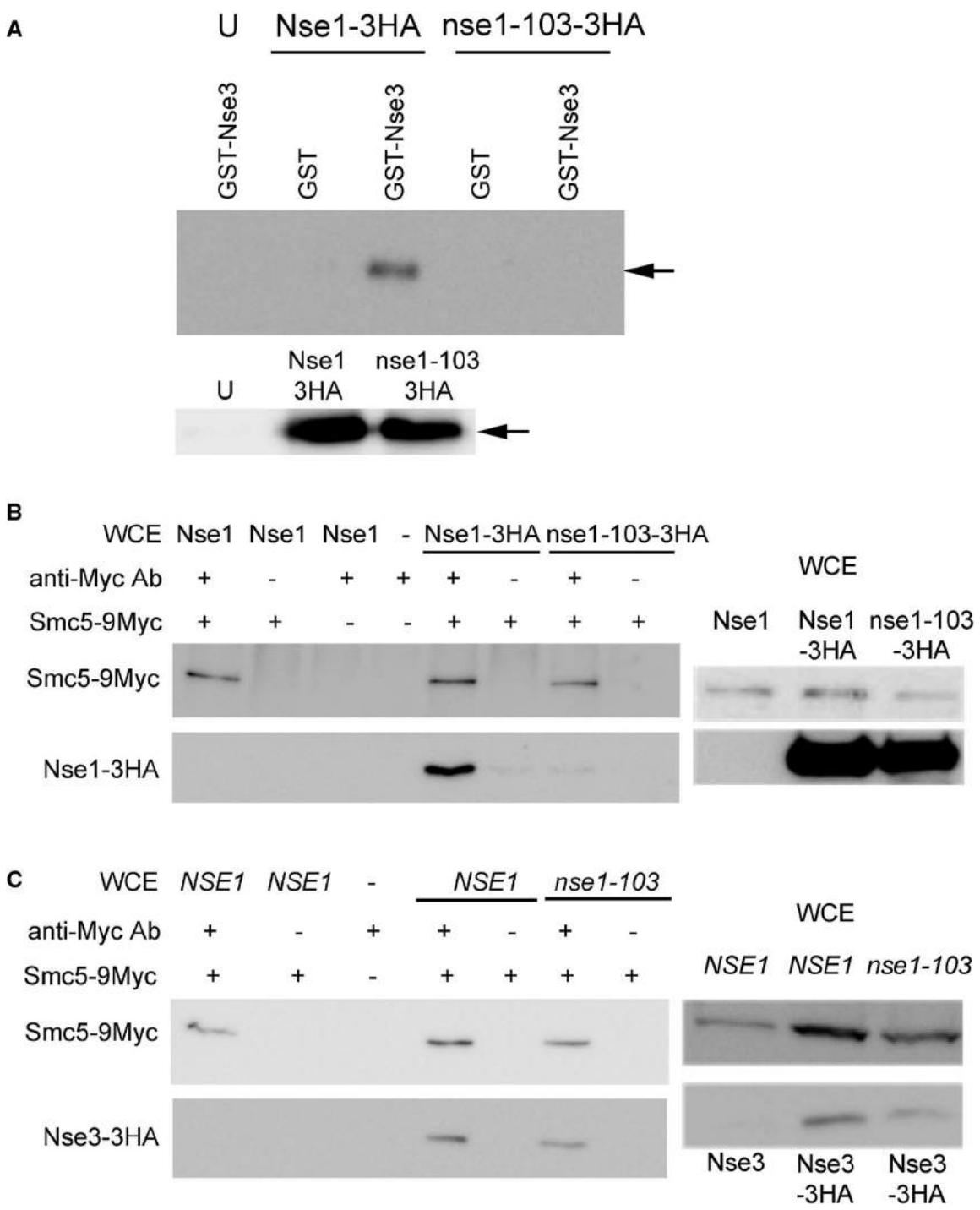

yWSS1572-1. Spontaneous chromosome loss events were enhanced significantly in *nse1-103* compared to wild-type cells in case of both the YACs, PA3-1 (Fig. 4b, bottom left graphs) (5.4-fold, $P = 0.0047$; unpaired two tailed *t*-test) and yWSS1572-1 (Fig. 4b, bottom right graphs) (2.5-fold, $P = 0.0502$), while chromosome breakage frequencies were unaltered (Fig. 4b, top graphs).

Decrease in sister chromatid cohesion in *nse1-103*

An enhanced chromosome loss phenotype may arise from defects in chromosome segregation. Sister chromatid cohesion is an important structural property of chromosomes that ensures their accurate segregation. We compared sister chromatid cohesion between wild-type and *nse1-103* mutant cells at a site on chromosome IV arm that has a lacO array that binds GFP-tagged lac-repressor resulting in a green

◂**Fig. 3** Analysis of inter-subunit interaction of Smc5/6 complex subunits in wild-type and *nse1-103* by physical assays. **a** Binding of recombinant GST–Nse3 on glutathione Sepharose resin to Nse1-3HA or nse1-103-3HA proteins from yeast cell extracts. Whole-cell extract from yeast strains expressing Nse1-3HA or nse1-103-3HA proteins (SLY2213 or SLY2214) was incubated with GST or GST–Nse3 bound resin. The top panel depicts the protein profile after eluting from the resin following western blotting using 12CA5 anti-HA antibody (1:5000 dilution) for the detection of wild-type or mutant Nse1-3HA. The lower western blot panel shows the level of Nse1-3HA or nse1-103-3HA proteins in the input from yeast cell extracts. U indicates extract having untagged Nse1 was used. **b** Co-immunoprecipitation to analyze binding of Nse1/nse1-103 with Smc5 in yeast cell extracts. Smc5 was immunoprecipitated using anti-MYC antibody from yeast cells expressing 9Myc-tagged Smc5 and 3HA-tagged Nse1 (SLY2491) or nse1-103 (SLY2492) or untagged Nse1 (SLY2318, a negative control). The immunoprecipitates were resolved by SDS–PAGE and analyzed by western blotting using anti-HA antibody to detect 3HA-tagged Nse1/nse1-103 associated with the Smc5/6 complex. The panels on the right are western blots of the input whole-cell extracts (WCE) from the cells expressing 9Myc-Smc5. (A)/Smc6 (B) in wild-type or *nse1-103* cells (**c**) Smc5 binds Nse3 in *nse1-103* mutant cells. Smc5 was immunoprecipitated from extracts of wild-type or *nse1-103* yeast cells expressing 9Myc-tagged Smc5 and 3HA-tagged Nse3 (SLY2565 and SLY2566). The samples were analyzed by western blotting to confirm Smc5-9Myc immunoprecipitation using anti-MYC antibody (top panel) and probed for Nse3-3HA co-immunoprecipitation using the anti-HA antibody (bottom panel). The panels on the right are results of western blot of the input whole-cell extracts showing 9Myc-Smc5 (top) and Nse3-3HA (bottom) levels in the cell lysates prepared from wild-type or *nse1-103* cells

fluorescent dot signal (Neurohr et al. 2011). The *nse1-103* mutation was introduced into a haploid strain having the GFP-tagged chromosome arm and cohesion or loss of cohesion was enumerated by quantifying the percentage of cells having one dot or two dots in nocodazole-arrested cells at 23 °C by confocal microscopy. The *nse1-103* mutant cells displayed a modest but statistically significant decrease in cohesion as evidenced by ~ 12.5% decrease in cells having one GFP signal (Fig. 5, left graph) versus a corresponding increase in cells having two GFP signals (Fig. 5, right graph) ($P = 0.004$; unpaired two tailed *t*-test).

Delayed completion of chromosomal replication is observed in *nse1-103* at elevated temperatures

To further investigate defects correlating with the slow growth and chromosome instability phenotypes of *nse1-103*, we synchronized wild-type and *nse1-103* mutant cells in G1 using alpha-factor and then released them from arrest into fresh medium at the restrictive temperature (34 °C, Fig. 6). Chromosomal DNA was analyzed at various time intervals after the release from arrest by pulsed-field gel electrophoresis. At twenty minutes after the release, there is decrease in the band intensities of chromosomes that have ongoing replication perhaps because of the accumulation of replication intermediates in the well, as expected (Fig. 6a). At forty and sixty minutes post release from arrest, an increase in the band intensity in the wild-type cells relative to G1 represents replication-dependent increase in DNA content. A dip at eighty minutes may correlate with completion of replication and entry into the next cycle. We observed that the *nse1-103* mutant cells initiate replication like wild-type cells but display a delay in doubling the DNA content particularly evident in case of the late replicating longer chromosomes IV(Fig. 6b, top graph) and XII (Fig. 6b, bottom graph) and in completion of replication. This indicates a role for Nse1 in progression and completion of replication.

Genetic interaction of *nse1-103* with replication defective mutants

Subunits of the Smc5/6 complex, Smc6 and Mms21 have been implicated in various aspects of DNA replication, such as rescue and restart of collapsed replication forks (Lindroos et al. 2006), resolution of recombination intermediates formed during recovery from DNA damage (Branzei et al. 2006) and prevention of damage at natural replication fork pausing sites (Menolfi et al. 2015). In an earlier study, a strain expressing S-phase-restricted Smc6 (that is not produced in G2/M) showed a synthetic sick phenotype with *rrm3*Δ, a mutant defective in Rrm3, a DNA helicase that facilitates fork passage through pausing sites or replication fork barriers (Menolfi et al. 2015). To test whether the delay in the completion of replication observed in *nse1-103* in our study may indicate its requirement in a similar process, we deleted *RRM3* in the *nse1-103* mutant. The *nse1-103 rrm3*Δ double mutant displayed a synthetic sick growth defect relative to either single mutant at 23 °C as well as 34 °C (Fig. 7a). Furthermore, deletion of *TOF1*, a gene encoding Tof1, a subunit of the replication-associated fork protection complex Tof1-Csm3 that enforces pausing at pausing sites, partially rescues the synthetic sickness of the *nse1-103 rrm3*Δ double mutant (Fig. 7b). We also deleted *MPH1*, that encodes an Smc5/6 complex-associated DNA helicase involved in a replication-associated recombination sub-pathway, in *nse1-103*, and found that its deletion partially alleviates the temperature sensitivity of the *nse1-103* mutant (Fig. 7c).

Homology modeling and comparison of ScNse1-Nse3 with human NSE1-MAGEG1

Doyle et al. reported the identification of human MAGE–RING complexes that are similar to Nse3-Nse1 in *S. cerevisiae* (Doyle et al. 2010). The crystal structure of the NSE1–MAGEG1 complex that is the homolog of Nse1–Nse3 was determined by them (Doyle et al. 2010). The structure revealed that the MHD (MAGE Homology Domain) of MAGEG1 forms a tandem winged helix andMAGEG1

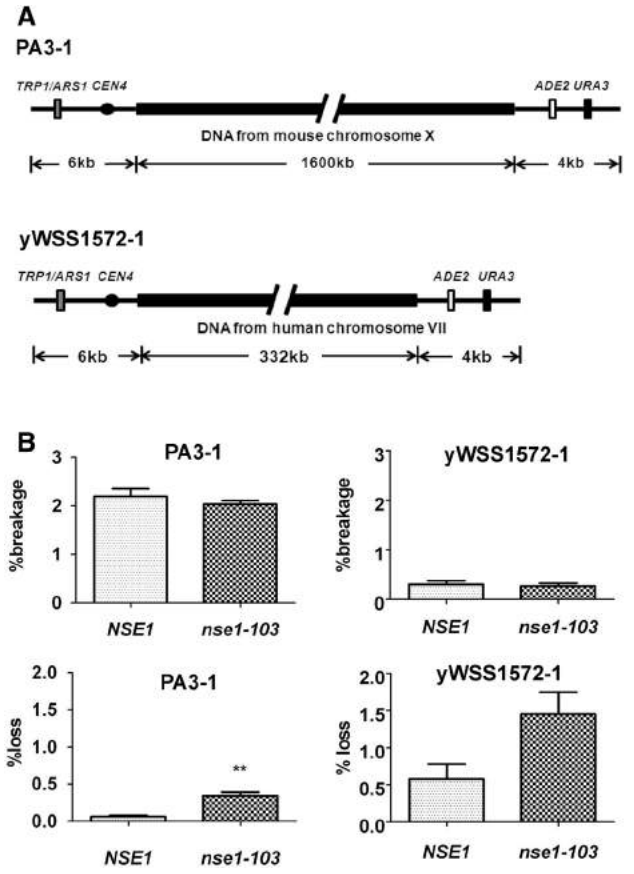

Fig. 4 Measurement of chromosome stability in wild-type and *nse1-103* mutant cells. **a** Quantitative genetic assay for measuring telomere marker loss (a measure of YAC breakage frequency) and YAC loss. The schematic shows the organization of the YACs used for the gross chromosomal rearrangement assay (adapted from Huang and Koshland 2003; Huang and Koshland 2003). **b** Chromosome instability in *nse1-103* cells grown at 23 °C. Quantification of telomere marker loss (YAC integrity; top panels) and total YAC loss (YAC stability; bottom panels) plotted as percent loss on the *y-axis* in WT (OR SLY2583 and SLY2571) and *nse1-103* (SLY2584 and SLY2572) cells that harbored the YACs PA3-I (left panels) and yWSS1572-1 (right panels) are shown. Error bars indicate standard error of the mean. The unpaired two-tailed Student's *t* test was used to evaluate the statistical significance; double asterisk indicates a statistically significant difference and implies a *P* value that is <0.01 ($P=0.0047$ in this case)

binds the N-terminal winged helix of NSE1. The structure also revealed that the RING domain of NSE1 indeed coordinates two Zn atoms. To deduce whether the budding yeast Nse1–Nse3 heterodimer has the potential to assume a structure similar to human NSE1–MAGEG1, we performed homology modeling of the ScNse1–Nse3 heterodimer using the known structure of human NSE1–MAGEG1 (Fig. 8a) as the template. The predicted model (Fig. 8b) revealed that ScNse1–Nse3 indeed has the potential to assume a structure retaining the core structural elements and overall similar organization as that of the NSE1–MAGEG1 heterodimer in humans. Interestingly, the positions of key conserved Zn-coordinating cysteine and histidine residues in the modeled Nse1–Nse3 heterodimer showed a striking coincidence with the spatially related conserved residues that coordinate the Zn atoms in the NSE1–MAGEG1 structure, including the ones substituted in *nse1-103*. This suggests that Nse1 in budding yeast also has the potential to coordinate Zn atoms to form its RING-domain like its human counterpart. Interestingly, the zinc-coordinating cluster is located away from the Nse1/3 interface in the predicted structure of yeast Nse1–Nse3 as well as the known structure of human NSE1–MAGEG1.

Discussion

We have investigated the role of the RING-domain of *Saccharomyces cerevisiae* Nse1 in Smc5/6 complex subunit association and in supporting its role in the maintenance of chromosome stability. The RING-domain is a structurally and functionally important domain in this class of proteins that has a C4HC3 consensus. Human NSE1 has been demonstrated to have a ubiquitin ligase activity (Doyle et al. 2010) that could not be demonstrated for fission yeast Nse1 (Pebernard et al. 2008).

Previous studies with fission yeast show that deletion of the Nse1 RING-domain reduced its interaction with Nse4 but not significantly with Nse3 (Pebernard et al. 2008). Here, we created more subtle substitution mutations in conserved residues of the budding yeast Nse1 RING-domain to investigate its role in Smc5/6 complex formation and function. Although single substitutions of C289, H306 or C309 with alanine did not result in any phenotypic defect, simultaneous substitution of H306 and C309 with alanine caused strong sensitivity to genotoxic agents and temperature. This mutant, *nse1-103*, produced a mutant protein in yeast cells that was surprisingly defective in binding Nse3 (unlike the case in fission yeast), as well as Nse4. The nse1-103 protein also did not interact with Smc5, whereas the interaction between Smc5 and Nse3 was preserved in the *nse1-103* mutant suggesting that interaction with Nse1 is dispensable for Nse3–Smc5 association.

A notable feature of the structure of the human MAGE–G1–NSE1 heterodimer is that the zinc-coordinating RING-domain of NSE1 is away from the MAGE-G1 and NSE1 interaction interface. However, intriguingly we found that substitution of H306 and C309 in the budding yeast Nse1 RING disrupted the interaction with Nse3. Given the potential structural similarity between the ScNse3–Nse1 heterodimer with MAGE-G1–NSE1 predicted by homology modeling (Fig. 8b), it is unlikely that the residues altered in nse1-103 form direct contact with the Nse3 interfacial residues important for stabilizing the

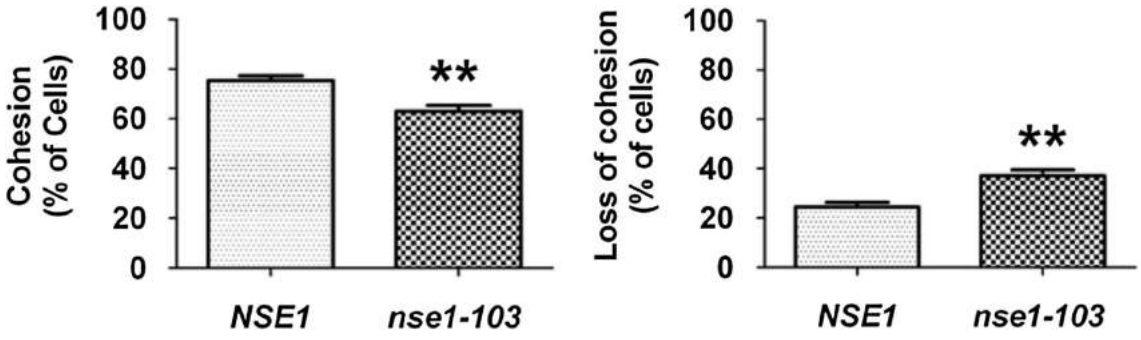

Fig. 5 Analysis of sister chromatid cohesion. Haploid wild-type or *nse1-103* mutant strains (WT SLY2646 and SLY2647) bearing a GFP-tagged chromosome arm site (having a lacO array integrated within *lys4* on chromosome IV in a strain expressing lacR-GFP) were arrested in mitosis using nocodazole (15 µg/ml). Images were captured by confocal microscopy and GFP fluorescence signals corresponding to cohesion (one dot) or lack of cohesion (two dots) were enumerated from approximately 100 nuclei per sample. The percent of cells showing cohesion (left graph) or no cohesion (right graph) are plotted on the Y-axis for wild-type (*NSE1*) and *nse1-103* cells. The unpaired two-tailed Student's *t* test was used to evaluate the statistical significance; double asterisk indicates a statistically significant difference and implies a *P* value that is <0.01 ($P=0.004$ in this case)

Nse3–Nse1 interaction. A closer look at the structure of the human NSE1–MAGEG1 heterodimer (Fig. 8a) may provide a clue to rationalize this confounding observation. The RING-domain of human NSE1 is connected to two key α-helices near the Nse1–Nse3 interface via two conserved β-sheets (Fig. 8a, indicated in red). Substitution of two zinc-coordinating residues within one cluster is likely to abrogate zinc binding and cause a severe disruption in the structure of the RING-domain that may then allosterically disrupt interfacial interactions between the conserved NSE1 alpha helical regions facing MAGE-G1/NSE3 via the distortion of the conserved connecting β-sheets. The predicted structural similarity of ScNse1–Nse3 to NSE1–MAGEG1 (Fig. 8b) by homology modeling includes preservation of the key structural modules and features referred to above, indicating this as a plausible mechanism also for allosteric disruption of ScNse1–Nse3 interaction by Nse1 RING domain mutations observed in this study.

We observed that Nse1 RING-domain dysfunction coupled with loss of interaction with other Smc5/6 subunits results in chromosome instability or enhanced frequency of chromosome loss. A possible cause of this may be reduction in sister chromatid cohesion as observed in our study that may result in unequal chromosome segregation. An overlap between Smc5/6 complex and cohesin chromosomal binding sites has been reported previously pointing to an intriguing connection between the two complexes. While Scc2, a component of the cohesin loading complex, is also required for binding of Smc5/6 (Lindroos et al. 2006), there have also been reports indicating a requirement for a functional Smc5/6 complex for cohesin binding to DSBs in human cells (Potts et al. 2006). Hence, it is possible that reduction in cohesion by a similar mechanism in the *nse1-103* mutant may partially contribute to the enhanced chromosome loss phenotype observed in our study.

We also observed that the RING-domain defective mutant exhibits a delay in the completion of chromosomal DNA replication, particularly evident in case of chromosome IV and XII, the largest yeast chromosomes, although replication of other chromosomes is also delayed to some extent. This may indicate that the Nse1 RING-domain supports the function of Smc5/6 in its various roles in replication, such as replication fork progression, rescue of stalled or collapsed forks and safe passage through replication pause sites or replication fork barriers. Menolfi et al. (Menolfi et al. 2015) have reported that origin firing and replication speed is not altered in strains expressing G2/M-restricted Smc5/6 indicating that the Smc5/6 complex is not critical for these events that occur in S-phase. However, in their study, S-phase limited expression of Smc5/6 complex subunits was associated with lethality (e.g. Smc5 and Nse4) or severe slow growth (e.g. Mms21 and Nse1) suggesting that the essential function of Smc5/6 is mainly in G2/M after bulk chromosome replication. Interestingly, *S-SMC6* cells (expressing S-phase-limited Smc6) were viable due to persistence of some amount of Smc6 protein in G2/M, that made genetic interaction studies (for identification of mutants that exhibit a synthetic sick phenotype with *S-SMC6*) feasible (Menolfi et al. 2015). They found that *S-SMC6* but not *G2-SMC6* was synthetic lethal/sick with *rrm3*, defective in Rrm3, a DNA helicase that promotes replication fork passage through natural pausing sites, at which the Smc5/6 complex binding is enriched (Menolfi et al. 2015). Deletion of *TOF1* that encodes a component of a replisome-associated fork protection complex that enforces pausing at these sites, rescued the synthetic sickness of *S-SMC6 rrm3*, indicating that prolonged pausing at these sites resulting in unfinished replication may

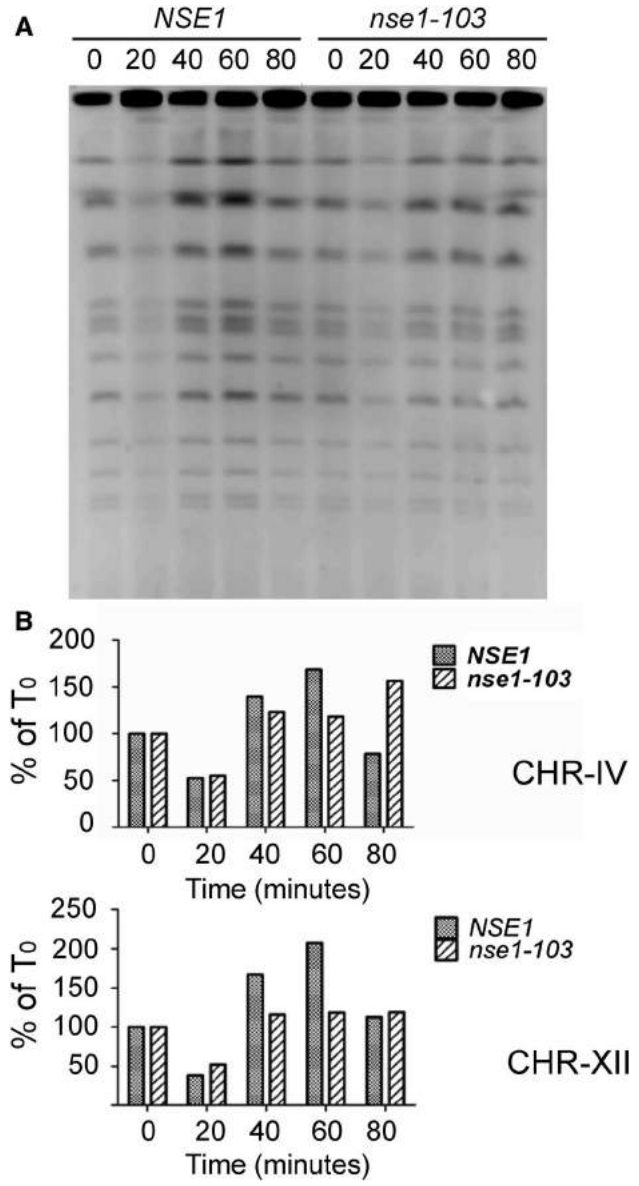

Fig. 6 Analysis of chromosomal DNA replication in wild-type and *nse1-103* cells. **a** Wild-type or *nse1-103* mutant cells (SLY2246 and SLY2247) were synchronized in G1 by alpha-factor and released from arrest at the indicated temperature (34 °C). Cells were harvested at the indicated time points (in minutes) and embedded in agarose plugs processed for in gel chromosome release that were resolved by pulsed-field gel electrophoresis (PFGE). **b** Quantification of the band intensities of the gel in A. Band intensities of chromosomes IV (top graphs) and XII (bottom graphs) for wild-type (gray bar) or mutant (hatched bar) were quantified after background subtraction and are normalized with respect to G1 cells (time 0), whose signal was set at 100%, shown on the *Y*-axis. Time in minutes is on the *X*-axis. Representative data are shown out of three independent experiments

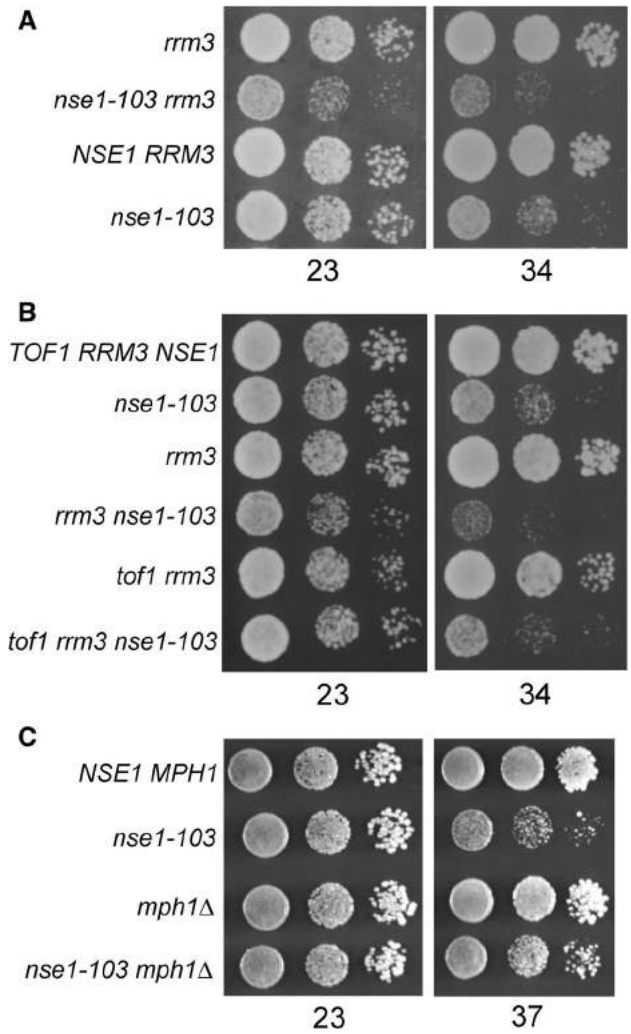

Fig. 7 Genetic interaction of *nse1-103* with replication factors. **a** Synthetic sick genetic interaction between *nse1-103* and *rrm3*Δ. Wild-type and various mutant strain cultures were normalized with respect to OD_{600}, serially diluted by 10-fold and spotted on YPD plates incubated at 23 °C (left panel) or 34 °C (right panel) in the order (from top to bottom) *rrm3*Δ, *rrm3*Δ *nse1-103*, WT or *NSE1 RRM3* and *nse1-103* (SLY2616, SLY2619, SLY1651 and SLY1653) **b** Suppression of the synthetic sickness of *rrm3*Δ *nse1-103*, by *tof1*Δ. Wild-type, single, double and triple mutant strains were spotted as described in A. The slow growth of *rrm3*Δ *nse1-103* (fourth row) is suppressed partially by a *tof1* deletion mutation. The strains included are (from top to bottom) wild-type, *nse1-103, rrm3*Δ, *rrm3*Δ *nse1-103, tof1*Δ *rrm3*Δ and *tof1*Δ *rrm3*Δ *nse1-103* (SLY1651, SLY1653, SLY2616, SLY2619, SLY2628 and SLY2631, respectively). **c** Suppression of the temperature sensitivity of *nse1-103* by *mph1*Δ. Serially diluted cultures of wild-type, *nse1-103, mph1Δ* and *nse1-103 mph1Δ* (SLY2246. SLY2247, SLY2768 and SLY2769) yeast strains were spotted on YPD plates and incubated at 23 or 37 °C for 2.5 days

cause the lethality in the *S-SMC6 rrm3* strain. A delay in the completion of replication of longer and late replicating chromosomes IV and XII [that also has the rDNA tandem array with a replication fork barrier (RFB) or pausing site in each repeat] was also noted in our analysis of the *nse1-103* mutant. Hence, we explored the genetic interaction of *nse1-103* with *rrm3Δ*; the double mutant *nse1-103 rrm3Δ* was synthetic sick and this sickness was indeed rescued partially by *tof1* deletion indicating that a similar mechanism

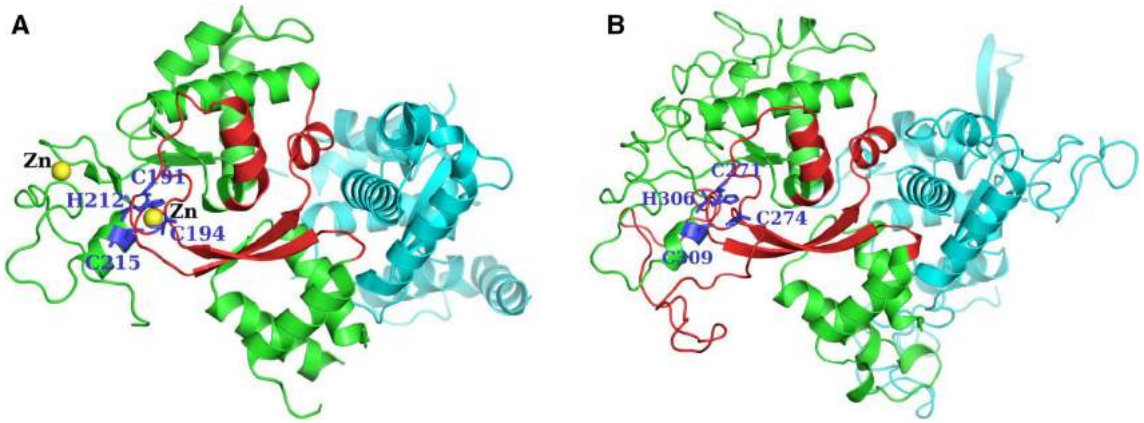

Fig. 8 Homology modeling of the structure of the *Saccharomyces cerevisiae* Nse1–Nse3 heterodimer. **a** The known structure of human NSE1–MAGEG1 heterodimer (3NW0). Ribbon depiction of various structural elements of NSE1 (green and red, on the left) and MAGEG1 (cyan, right). The two yellow spheres represent the zinc atoms of the zinc-coordinating cluster. His212 and Cys215 are equivalent to the residues mutated in the *nse1-103* mutant characterized by us in this study. **b** Predicted structure of budding yeast Nse1–Nse3 heterodimer obtained by homology modeling, showing overall similarity in organization and conservation of key structural elements with the human counterpart. The red regions in the yeast structure correspond to residues 77–151 (beta sheet followed by helix) and 256–278 (helix followed by a loop). In both structures, the affected zinc-coordinating cluster that may be disrupted in the mutant is connected via 2 β-sheets to two interfacial alpha helices (shown in red) facing the NSE1–MAGEG1/Nse3 interface

in which prolonged pausing at RFBs delays completion of replication may also occur in the *nse1-103* RING domain mutant defective in association with other Smc5/6 complex subunits, that may culminate in enhanced loss of such incompletely replicated chromosomes.

Our study reveals a requirement for the *S. cerevisiae* Nse1 RING-domain containing subunit in maintenance of chromosome stability. Interaction of Nse1 with other Smc5/6 complex subunits is important for the completion of replication and sister-chromatid cohesion that are impaired in an Nse1 RING-domain defective mutant; mis-regulation of these two important chromosomal processes may cause chromosome instability as observed in our study and may explain similar phenotypes associated with Smc5/6 complex dysfunction in human disease (van der Crabben et al. 2016) and model organisms.

Acknowledgements This work was supported by investigator specific grants to Shikha Laloraya from the Science and Engineering Research Board (SERB), Department of Biotechnology (DBT) and Council of Scientific and Industrial Research (CSIR), India, and the DBT-IISc partnership program funded by the Department of Biotechnology, India. Fellowship support for Saima Wani was provided by the Indian Institute of Science and the SERB grant to S.L. Deepash Kothiwal was supported by a Department of Biotechnology Senior Research Fellowship, Lakshmi Mahendrawada by the CSIR grant to S.L., and Neelam Maharshi by a fellowship from I.I.Sc. We thank Yves Barral, Kenji Kohno and Doug Koshland for sharing strains and plasmids, Donald Soubam for construction of pDS58 and pDS72, Deepa Balagopal for construction of pDB30, and N. Srinivasan for discussions related to the structure. Technical support from the DBT funded confocal facility of I.I.Sc. is acknowledged. Equipment support for the Department of Biochemistry, I.I.Sc. is provided by the DST-FIST and UGC CAS/SAP programs.

Author contributions S.M. and S.L. designed the experiments. S.M., N.M., L.M. and D.K. performed the experiments. S.M., N.M., D.K., L.M. and S.L. analyzed the data. S.L. performed the homology modeling and K.R. analyzed and interpreted the Nse1/3 heterodimer model. S.L. designed and supervised the project and wrote the manuscript. All authors reviewed the results and approved the final version of the manuscript.

Compliance with ethical standards

Conflict of interest The authors declare that they have no conflicts of interest with the contents of this article.

References

Ampatzidou E, Irmisch A, O'Connell MJ, Murray JM (2006) Smc5/6 is required for repair at collapsed replication forks. Mol Cell Biol 26:9387–9401. https://doi.org/10.1128/MCB.01335-06

Arnold K, Bordoli L, Kopp J, Schwede T (2006) The SWISS-MODEL workspace: a web-based environment for protein structure homology modelling. Bioinformatics 22:195–201. https://doi.org/10.1093/bioinformatics/bti770

Bahler J, Wu JQ, Longtine MS, Shah NG, McKenzie A 3rd, Steever AB, Wach A, Philippsen P, Pringle JR (1998) Heterologous modules for efficient and versatile PCR-based gene targeting in *Schizosaccharomyces pombe*. Yeast 14:943–951. https://doi.org/10.1002/(SICI)1097-0061(199807)14:10<943::AID-YEA292>3.0.CO;2-Y

Benkert P, Biasini M, Schwede T (2011) Toward the estimation of the absolute quality of individual protein structure models. Bioinformatics 27:343–350. https://doi.org/10.1093/bioinformatics/btq662

Bermudez-Lopez M, Aragon L (2017) Smc5/6 complex regulates Sgs1 recombination functions. Curr Genet 63:381–388. https://doi.org/10.1007/s00294-016-0648-5

Biasini M, Bienert S, Waterhouse A, Arnold K, Studer G, Schmidt T, Kiefer F, Gallo Cassarino T, Bertoni M, Bordoli L, Schwede T (2014) SWISS-MODEL: modelling protein tertiary and

quaternary structure using evolutionary information. Nucleic Acids Res 42:W252-258. https://doi.org/10.1093/nar/gku340
Borden KL, Freemont PS (1996) The RING finger domain: a recent example of a sequence-structure family. Curr Opin Struct Biol 6:395–401 doi
Branzei D, Foiani M (2009) The checkpoint response to replication stress. DNA Repair (Amst) 8:1038–1046. https://doi.org/10.1016/j.dnarep.2009.04.014
Branzei D, Foiani M (2010) Maintaining genome stability at the replication fork. Nat Rev Mol Cell Biol 11:208–219. https://doi.org/10.1038/nrm2852
Branzei D, Sollier J, Liberi G, Zhao X, Maeda D, Seki M, Enomoto T, Ohta K, Foiani M (2006) Ubc9- and mms21-mediated sumoylation counteracts recombinogenic events at damaged replication forks. Cell 127:509–522. https://doi.org/10.1016/j.cell.2006.08.050
Bustard DE, Menolfi D, Jeppsson K, Ball LG, Dewey SC, Shirahige K, Sjogren C, Branzei D, Cobb JA (2012) During replication stress, non-SMC element 5 (NSE5) is required for Smc5/6 protein complex functionality at stalled forks. J Biol Chem 287:11374–11383. https://doi.org/10.1074/jbc.M111.336263
Bustard DE, Ball LG, Cobb JA (2016) Non-Smc element 5 (Nse5) of the Smc5/6 complex interacts with SUMO pathway components. Biol Open 5:777–785. https://doi.org/10.1242/bio.018440
De Piccoli G, Cortes-Ledesma F, Ira G, Torres-Rosell J, Uhle S, Farmer S, Hwang JY, Machin F, Ceschia A, McAleenan A, Cordon-Preciado V, Clemente-Blanco A, Vilella-Mitjana F, Ullal P, Jarmuz A, Leitao B, Bressan D, Dotiwala F, Papusha A, Zhao X, Myung K, Haber JE, Aguilera A, Aragon L (2006) Smc5-Smc6 mediate DNA double-strand-break repair by promoting sister-chromatid recombination. Nat Cell Biol 8:1032–1034. https://doi.org/10.1038/ncb1466
De Piccoli G, Torres-Rosell J, Aragon L (2009) The unnamed complex: what do we know about Smc5-Smc. 6? Chromosome Res 17:251–263. https://doi.org/10.1007/s10577-008-9016-8
Ding DQ, Haraguchi T, Hiraoka Y (2016) A cohesin-based structural platform supporting homologous chromosome pairing in meiosis. Curr Genet 62:499–502. https://doi.org/10.1007/s00294-016-0570-x
Doyle JM, Gao J, Wang J, Yang M, Potts PR (2010) MAGE-RING protein complexes comprise a family of E3 ubiquitin ligases. Mol Cell 39:963–974. https://doi.org/10.1016/j.molcel.2010.08.029
Duan X, Sarangi P, Liu X, Rangi GK, Zhao X, Ye H (2009a) Structural and functional insights into the roles of the Mms21 subunit of the Smc5/6 complex. Mol Cell 35:657–668. https://doi.org/10.1016/j.molcel.2009.06.032
Duan X, Yang Y, Chen YH, Arenz J, Rangi GK, Zhao X, Ye H (2009b) Architecture of the Smc5/6 Complex of *Saccharomyces cerevisiae* Reveals a Unique Interaction between the Nse5-6 Subcomplex and the Hinge Regions of Smc5 and Smc6. J Biol Chem 284:8507–8515. https://doi.org/10.1074/jbc.M809139200
Fujioka Y, Kimata Y, Nomaguchi K, Watanabe K, Kohno K (2002) Identification of a novel non-structural maintenance of chromosomes (SMC) component of the SMC5-SMC6 complex involved in DNA repair. J Biol Chem 277:21585–21591. https://doi.org/10.1074/jbc.M201523200
Guex N, Peitsch MC, Schwede T (2009) Automated comparative protein structure modeling with SWISS-MODEL and Swiss-PdbViewer: a historical perspective. Electrophoresis 30 Suppl 1: S162-173 https://doi.org/10.1002/elps.200900140
Hartwell LH, Kastan MB (1994) Cell cycle control and cancer. Science 266:1821–1828 doi
Harvey SH, Sheedy DM, Cuddihy AR, O'Connell MJ (2004) Coordination of DNA damage responses via the Smc5/Smc6 complex. Mol Cell Biol 24:662–674 doi
Hirano T (2016) Condensin-based chromosome organization from bacteria to vertebrates. Cell 164:847–857. https://doi.org/10.1016/j.cell.2016.01.033
Huang D, Koshland D (2003) Chromosome integrity in *Saccharomyces cerevisiae*: the interplay of DNA replication initiation factors, elongation factors, and origins. Genes Dev 17:1741–1754. https://doi.org/10.1101/gad.1089203
Iadonato SP, Gnirke A (1996) RARE-cleavage analysis of YACs. Methods Mol Biol 54:75–85 doi
Iwasaki O, Noma KI (2016) Condensin-mediated chromosome organization in fission yeast. Curr Genet 62:739–743. https://doi.org/10.1007/s00294-016-0601-7
Janke C, Magiera MM, Rathfelder N, Taxis C, Reber S, Maekawa H, Moreno-Borchart A, Doenges G, Schwob E, Schiebel E, Knop M (2004) A versatile toolbox for PCR-based tagging of yeast genes: new fluorescent proteins, more markers and promoter substitution cassettes. Yeast 21:947–962. https://doi.org/10.1002/yea.1142
Jeppsson K, Kanno T, Shirahige K, Sjogren C (2014) The maintenance of chromosome structure: positioning and functioning of SMC complexes. Nat Rev Mol Cell Biol 15:601–614. https://doi.org/10.1038/nrm3857
Kaelin WG Jr, Krek W, Sellers WR, DeCaprio JA, Ajchenbaum F, Fuchs CS, Chittenden T, Li Y, Farnham PJ, Blanar MA et al (1992) Expression cloning of a cDNA encoding a retinoblastoma-binding protein with E2F-like properties. Cell 70:351–364 doi
Kiefer F, Arnold K, Kunzli M, Bordoli L, Schwede T (2009) The SWISS-MODEL Repository and associated resources. Nucleic Acids Res 37:D387-392. https://doi.org/10.1093/nar/gkn750
Koshland D, Strunnikov A (1996) Mitotic chromosome condensation. Annu Rev Cell Dev Biol 12:305–333. https://doi.org/10.1146/annurev.cellbio.12.1.305
Kushnirov VV (2000) Rapid and reliable protein extraction from yeast. Yeast 16:857–860. https://doi.org/10.1002/1097-0061(20000630)16:9<857::AID-YEA561>3.0.CO;2-B
Leung GP, Lee L, Schmidt TI, Shirahige K, Kobor MS (2011) Rtt107 is required for recruitment of the SMC5/6 complex to DNA double strand breaks. J Biol Chem 286:26250–26257. https://doi.org/10.1074/jbc.M111.235200
Lindroos HB, Strom L, Itoh T, Katou Y, Shirahige K, Sjogren C (2006) Chromosomal association of the Smc5/6 complex reveals that it functions in differently regulated pathways. Mol Cell 22:755–767. https://doi.org/10.1016/j.molcel.2006.05.014
Losada A, Hirano T (2005) Dynamic molecular linkers of the genome: the first decade of SMC proteins. Genes Dev 19:1269–1287. https://doi.org/10.1101/gad.1320505
Mahendrawada L, Rai R, Kothiwal D, Laloraya S (2017) Interplay between Top1 and Mms21/Nse2 mediated sumoylation in stable maintenance of long chromosomes. Curr Genet 63:627–645. https://doi.org/10.1007/s00294-016-0665-4
Matityahu A, Onn I (2017) A new twist in the coil: functions of the coiled-coil domain of structural maintenance of chromosome (SMC) proteins. Curr Genet. https://doi.org/10.1007/s00294-017-0735-2
McDonald WH, Pavlova Y, Yates JR 3rd, Boddy MN (2003) Novel essential DNA repair proteins Nse1 and Nse2 are subunits of the fission yeast Smc5-Smc6 complex. J Biol Chem 278:45460–45467. https://doi.org/10.1074/jbc.M308828200
Menolfi D, Delamarre A, Lengronne A, Pasero P, Branzei D (2015) Essential Roles of the Smc5/6 Complex in Replication through Natural Pausing Sites and Endogenous DNA Damage Tolerance. Mol Cell 60:835–846. https://doi.org/10.1016/j.molcel.2015.10.023
Neurohr G, Naegeli A, Titos I, Theler D, Greber B, Diez J, Gabaldon T, Mendoza M, Barral Y (2011) A midzone-based ruler adjusts chromosome compaction to anaphase spindle length. Science 332:465–468. https://doi.org/10.1126/science.1201578

Palecek J, Vidot S, Feng M, Doherty AJ, Lehmann AR (2006) The Smc5-Smc6 DNA repair complex. bridging of the Smc5-Smc6 heads by the KLEISIN, Nse4, and non-Kleisin subunits. J Biol Chem 281:36952–36959. https://doi.org/10.1074/jbc.M608004200

Pebernard S, McDonald WH, Pavlova Y, Yates JR 3rd, Boddy MN (2004) Nse1, Nse2, and a novel subunit of the Smc5-Smc6 complex, Nse3, play a crucial role in meiosis. Mol Biol Cell 15:4866–4876. https://doi.org/10.1091/mbc.E04-05-0436

Pebernard S, Perry JJ, Tainer JA, Boddy MN (2008) Nse1 RING-like domain supports functions of the Smc5-Smc6 holocomplex in genome stability. Mol Biol Cell 19:4099–4109. https://doi.org/10.1091/mbc.E08-02-0226

Pfander B, Moldovan GL, Sacher M, Hoege C, Jentsch S (2005) SUMO-modified PCNA recruits Srs2 to prevent recombination during S phase. Nature 436:428–433. https://doi.org/10.1038/nature03665

Pickart CM (2001) Mechanisms underlying ubiquitination. Annu Rev Biochem 70:503–533. https://doi.org/10.1146/annurev.biochem.70.1.503

Potts PR, Porteus MH, Yu H (2006) Human SMC5/6 complex promotes sister chromatid homologous recombination by recruiting the SMC1/3 cohesin complex to double-strand breaks. EMBO J 25:3377–3388. https://doi.org/10.1038/sj.emboj.7601218

Prakash S, Prakash L (1977) Increased spontaneous mitotic segregation in MMS-sensitive mutants of Saccharomyces cerevisiae. Genetics 87:229–236 doi

Putnam CD, Srivatsan A, Nene RV, Martinez SL, Clotfelter SP, Bell SN, Somach SB, de Souza JE, Fonseca AF, de Souza SJ, Kolodner RD (2016) A genetic network that suppresses genome rearrangements in *Saccharomyces cerevisiae* and contains defects in cancers. Nat Commun 7:11256. https://doi.org/10.1038/ncomms11256

Rai R, Laloraya S (2017) Genetic evidence for functional interaction of Smc5/6 complex and Top1 with spatial frequency of replication origins required for maintenance of chromosome stability. Curr Genet 63:765–776. https://doi.org/10.1007/s00294-017-0680-0

Rai R, Varma SP, Shinde N, Ghosh S, Kumaran SP, Skariah G, Laloraya S (2011) Small ubiquitin-related modifier ligase activity of Mms21 is required for maintenance of chromosome integrity during the unperturbed mitotic cell division cycle in *Saccharomyces cerevisiae*. J Biol Chem 286:14516–14530. https://doi.org/10.1074/jbc.M110.157149

Rankin S, Dawson DS (2016) Recent advances in cohesin biology. F1000Res. https://doi.org/10.12688/f1000research.8881.1

Robellet X, Vanoosthuyse V, Bernard P (2016) The loading of condensin in the context of chromatin. Curr Genet. https://doi.org/10.1007/s00294-016-0669-0

Santa Maria SR, Gangavarapu V, Johnson RE, Prakash L, Prakash S (2007) Requirement of Nse1, a subunit of the Smc5-Smc6 complex, for Rad52-dependent postreplication repair of UV-damaged DNA in *Saccharomyces cerevisiae*. Mol Cell Biol 27:8409–8418. https://doi.org/10.1128/MCB.01543-07

Skibbens RV (2016) Of Rings and Rods: Regulating Cohesin Entrapment of DNA to Generate Intra- and Intermolecular Tethers. PLoS Genet 12:e1006337. https://doi.org/10.1371/journal.pgen.1006337

Tapia-Alveal C, O'Connell MJ (2011) Nse1-dependent recruitment of Smc5/6 to lesion-containing loci contributes to the repair defects of mutant complexes. Mol Biol Cell 22:4669–4682. https://doi.org/10.1091/mbc.E11-03-0272

Uhlmann F (2016) SMC complexes: from DNA to chromosomes. Nat Rev Mol Cell Biol 17:399–412. https://doi.org/10.1038/nrm.2016.30

van der Crabben SN, Hennus MP, McGregor GA, Ritter DI, Nagamani SC, Wells OS, Harakalova M, Chinn IK, Alt A, Vondrova L, Hochstenbach R, van Montfrans JM, Terheggen-Lagro SW, van Lieshout S, van Roosmalen MJ, Renkens I, Duran K, Nijman IJ, Kloosterman WP, Hennekam E, Orange JS, van Hasselt PM, Wheeler DA, Palecek JJ, Lehmann AR, Oliver AW, Pearl LH, Plon SE, Murray JM, van Haaften G (2016) Destabilized SMC5/6 complex leads to chromosome breakage syndrome with severe lung disease. J Clin Invest 126:2881–2892. https://doi.org/10.1172/JCI82890

Wehrkamp-Richter S, Hyppa RW, Prudden J, Smith GR, Boddy MN (2012) Meiotic DNA joint molecule resolution depends on Nse5-Nse6 of the Smc5-Smc6 holocomplex. Nucleic Acids Res 40:9633–9646. https://doi.org/10.1093/nar/gks713

Zhao X, Blobel G (2005) A SUMO ligase is part of a nuclear multiprotein complex that affects DNA repair and chromosomal organization. Proc Natl Acad Sci USA 102:4777–4782. https://doi.org/10.1073/pnas.0500537102